

6-6-2016

Mitigation of Radiation-Induced Bone Loss by Dried Plum

Carlos Medina
Santa Clara Univeristy

Sonette Steczina
Santa Clara Univeristy

Follow this and additional works at: http://scholarcommons.scu.edu/bioe_senior

Recommended Citation

Medina, Carlos and Steczina, Sonette, "Mitigation of Radiation-Induced Bone Loss by Dried Plum" (2016). *Bioengineering Senior Theses*. Paper 49.

This Thesis is brought to you for free and open access by the Student Scholarship at Scholar Commons. It has been accepted for inclusion in Bioengineering Senior Theses by an authorized administrator of Scholar Commons. For more information, please contact rsccroggin@scu.edu.

SANTA CLARA UNIVERSITY

Department of Bioengineering

I HEREBY RECOMMEND THAT THE THESIS PREPARED UNDER MY SUPERVISION
BY

Carlos Medina*, Sonette Steczina*



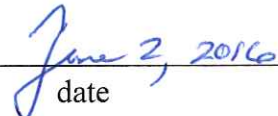




*Authors made equal contribution to this project

ENTITLED

Mitigation of Radiation-Induced Bone Loss by Dried Plum

BE ACCEPTED IN PARTIAL FULFILLMENT OF THE REQUIREMENTS
FOR THE DEGREE OF

**BACHELOR OF SCIENCE
IN
BIOENGINEERING**

| | | |
|---|---|---|
|  |  |  |
| Thesis Advisor | | date |
|  | |  |
| Thesis Advisor | | date |
|  | |  |
| Department Chair | | date |

Mitigation of Radiation-Induced Bone Loss by Dried Plum

By

Carlos Medina*, Sonette Steczina*

*Authors made equal contribution to this project

SENIOR DESIGN PROJECT REPORT

Submitted to
the Department of Bioengineering

of

SANTA CLARA UNIVERSITY

in Partial Fulfillment of the Requirements
for the degree of
Bachelor of Science in Bioengineering

Santa Clara, California

June 09, 2016

Abstract

In recent years, much attention has been given to the effects of radiation on bone deterioration. Past research has demonstrated that radiation acts to alter the balance between osteoblasts and osteoclasts, promoting a net osteoclastic activity in the affected bone tissue, but specific molecular mechanisms remain unknown. Gene expression of many osteoclast markers is upregulated early in response to radiation, leading to bone resorption. This problem is especially prominent in space, as astronauts are regularly exposed to full body ionizing radiation that, over extended periods of time, may lead to significant bone loss. Research suggests that radiation leads to an inflammatory response in bone tissue, which leads to oxidative stress damage and increased osteoclast activity. Numerous natural compounds have been studied *in vitro* and have been observed to reduce the gene expression of bone resorption genes and their protein derivatives. We have attempted to take a closer look at the mechanisms by which radiation impairs bone health by examining the microarchitecture of mouse bones and the gene expression of osteoclast, osteoblast, and osteocyte markers. Much research has been devoted to studying osteoclastic activity because this is believed to play the most influential role in bone loss. Our gene expression findings show that radiation increases bone resorption and oxidative stress. Oxidative damage analysis indicated a higher level of malondialdehyde (MDA) in the irradiated, control diet samples compared to non-irradiated mice on the control diet and suggested that dried plum may protect bones by a systemic reduction in oxidative damage. Physical characterization results that we obtained from microCT demonstrate that a dried plum diet increased the bone mass compared to the control diet, but failed to show an effect from radiation on bone. The microCT data collected is not sufficient to confirm that dried plum has a radio-protective effect in vertebrae. Although at this stage, we have limited data to fully understand the mechanisms by which dried plum protects bone, we show that dried plum can increase bone mass in vertebrae and systemically reduces MDA levels in circulation. Our research increases the current medical and biological understanding of bone physiology in response to radiation and proposed dietary countermeasures, and is of relevance to astronauts in extended space missions, cancer patients, and patients with osteoporosis.

Keywords: osteoblast, osteoclast, resorption, oxidative stress, qPCR, malondialdehyde, microCT, BV/TV, Tb.Th.

Acknowledgements

We would like to express our gratitude towards Dr. Ruth Globus and Dr. Candice Tahimic, for their instrumental guidance throughout this project and their willingness to allow us to conduct our research project at NASA Ames Research Center.

We would also like to thank Dr. Ann-Sofie Schreurs and Josergio Zaragoza at the Bone and Signaling Laboratory of NASA Ames, with whom we most directly worked, for their invaluable instruction, guidance, and advice for our research project.

Last but not least, we would also like to thank Dr. Prashanth Asuri at Santa Clara University for introducing us to the research opportunity at NASA, being our on-campus research advisor, and providing us with support and advice for our presentation and thesis throughout the year.

Thank you very much!!

Table of Contents

| | |
|--|-----|
| Abstract..... | iii |
| Acknowledgements..... | iv |
| List of Figures..... | 8 |
| List of Tables..... | 10 |
| List of Abbreviations..... | 11 |
| 1. Introduction..... | 12 |
| 1.1 Background and Motivation..... | 12 |
| 1.2 Relevant Literature Review..... | 13 |
| 1.2.1 Harmful Effects of Ionizing Radiation..... | 13 |
| 1.2.2 Measuring Radiation..... | 14 |
| 1.2.3 Space Radiation Environment..... | 14 |
| 1.2.4 The Skeletal System..... | 15 |
| 1.2.5 Characteristics and Functions of Osteoblasts & Osteoclasts..... | 16 |
| 1.2.6 Radiation Damage to Bone & Oxidative Stress..... | 17 |
| 1.2.7 Protective Effects of Dried Plum on the Skeleton..... | 18 |
| 1.2.8 Effects of Dried Plum Diet on Osteoblast & Osteoclast Gene Expression..... | 21 |
| 1.2.9 Other Natural Compounds..... | 23 |
| 1.3 Current Therapies..... | 25 |
| 1.4 Project Goals and Experimental Design..... | 26 |
| 1.5 Significance..... | 26 |
| 1.6 Team and Management..... | 27 |
| 1.6.1 Budget..... | 27 |
| 1.6.2 Timeline..... | 27 |
| 2. System Level Experimental Design..... | 29 |
| 2.1 System Level Overview..... | 29 |
| 2.2 System Level Constraints..... | 32 |
| 2.3 Experimental Approach..... | 34 |
| 2.4 Engineering Standards and Realistic Constraints..... | 35 |
| 3. Design Description..... | 38 |
| 3.1 Design Overview..... | 38 |

| | |
|------------------------------------|----|
| 3.2 Expected Results | 40 |
| 4. Historical System Setup | 42 |
| 4.1 Introduction..... | 42 |
| 4.2 Design Description..... | 42 |
| 4.3 Methods and Materials..... | 42 |
| 4.3.1 Dried Plum + 2Gy Gamma | 43 |
| 4.3.2 Dried Plum + 1Gy Iron | 43 |
| 4.4 Results..... | 44 |
| 4.4.1 Dried Plum + 2Gy Gamma | 44 |
| 4.4.2 Dried Plum + 1Gy Iron | 45 |
| 5. RNA Extraction from Bone | 46 |
| 5.1 Introduction..... | 46 |
| 5.2 Key Constraints..... | 46 |
| 5.3 Design Description..... | 46 |
| 5.4 Methods and Materials..... | 47 |
| 5.5 Results and Discussion | 47 |
| 6. RNA Conversion to cDNA | 50 |
| 6.1 Introduction..... | 50 |
| 6.2 Key Constraints..... | 50 |
| 6.3 Design Description..... | 50 |
| 6.4 Methods and Materials..... | 51 |
| 6.5 Results and Discussion | 51 |
| 7. Gene Expression Analysis | 52 |
| 7.1 Introduction..... | 52 |
| 7.2 Key Constraints..... | 53 |
| 7.3 Design Description..... | 53 |
| 7.4 Methods and Materials..... | 53 |
| 7.5 Results and Discussion | 54 |
| 8. Oxidative Damage Analysis | 59 |
| 8.1 Introduction..... | 59 |
| 8.2 Key Constraints..... | 60 |
| 8.3 Design Description..... | 60 |
| 8.4 Methods and Materials..... | 61 |

| | |
|--|----|
| 8.5 Results and Discussion | 61 |
| 9. Micro-Computed Tomography | 64 |
| 9.1 Introduction..... | 64 |
| 9.2 Key Restraints..... | 65 |
| 9.3 Design Description..... | 67 |
| 9.4 Methods and Materials..... | 67 |
| 9.4.1 Step 1: Scanning | 67 |
| 9.4.2 Step 2: Bone Reconstruction..... | 68 |
| 9.4.3 Step 3: Rotating/Re-alignment..... | 68 |
| 9.4.4 Step 4: Contouring | 68 |
| 9.4.5 Step 5: Quantification | 69 |
| 9.4.6 Step 6: Final 3D Image Generation..... | 70 |
| 9.5 Results & Discussion | 70 |
| 9.5.1 Quantification | 70 |
| 9.5.2 3D Images | 72 |
| 10. Conclusions..... | 75 |
| 10.1 Summary | 75 |
| 10.2 Future Work..... | 75 |
| 10.3 Concluding Remarks..... | 76 |
| 11. Appendices..... | 78 |
| 12. References..... | 93 |

List of Figures

| | <u>Page</u> |
|---|-------------|
| Figure 1 – Timeline of experiments. | 13 |
| Figure 2 – Skeletal development progression and patterning. [5] | 15 |
| Figure 3 – MicroCT images of trabecular bone. [2] | 17 |
| Figure 4 – Radiation and hindlimb unloading effects on lipid peroxidation. [3] | 18 |
| Figure 5 – BMD results of dried plum acting on the effects of orchidectomy (ORX). [7] | 19 |
| Figure 6 – Changes in BV/TV of tibia in OVX mice in response to various dietary supplements. [8] | 19 |
| Figure 7 – Dried Plum prevents bone loss induced by radiation. | 20 |
| Figure 8 – Effect on varying phenolic acids on ALP expression from rat serum. [11] | 21 |
| Figure 9 – Overview of experiments we undertook for our senior design project. | 29 |
| Figure 10 – Results from Bioanalyzer gel for 31 RNA samples indicating RNA integrity. | 48 |
| Figure 11 – Raw qPCR data reported by 7300 RT-PCR System analyzed for gene expression information. | 55 |
| Figure 12 – Gene expression of bone related genes in bone marrow cells. | 56 |
| Figure 13 – Gene expression of oxidative stress, DNA damage, and cell cycle related genes in bone marrow cells. | 57 |
| Figure 14 – Gene expression of bone related genes in mineralized midshaft bone samples. | 57 |
| Figure 15 – Gene expression of oxidative stress, DNA damage, and cell cycle related genes in mineralized midshaft bone samples. | 58 |
| Figure 16 – TBARS preliminary experiment for dilution determination. | 62 |
| Figure 17 – TBARS for Serum samples. | 62 |
| Figure 18 – Lumbar Vertebrae highlighting important locations and directions. | 64 |
| Figure 19 – Lumbar 4 vertebrae with region of interest highlighted within the vertebral body. | 69 |
| Figure 20 – Quantitative morphometry data determined by microCT for vertebrae (appendicular skeleton). | 71 |
| Figure 21 – Quantitative morphometry data determined by microCT for tibia (axial skeleton). | 72 |
| Figure 22 – Representative images of 3D reconstruction of cancellous bone micro-architecture via microCT. | 73 |

Figure 23 – Excel spreadsheet utilized to calculate qPCR "recipe" for 31 samples and 1 gene of interest. 87

Figure 24 – Set up for the 96 well and 384 well plates utilized for qPCR of 31 samples and 1 gene of interest from the 'Dried plum + 2Gy gamma' experiment. 88

List of Tables

| | <u>Page</u> |
|---|-------------|
| Table 1 – Results of RNA concentrations (ng/uL) for each RNA sample (‘Dried plum + 2Gy gamma’ experiment) via NanoDrop and accompanying RIN#'s via Bioanalyzer. | 49 |
| Table 2 – Complete itemized estimated costs for all reagents utilized for our experiments. | 78 |
| Table 3 - Assigned diet and radiation condition for all mice from ‘Dried plum + 2Gy gamma’ experiment. | 79 |
| Table 4 - Assigned diet and radiation condition for all mice from ‘Dried plum + 1Gy Iron’ experiment. | 80 |
| Table 5 - Table of all genes we analyzed during the course of our project during the gene expression phase. | 89 |
| Table 6 - Table of all parameters of interest that were analyzed after performing microCT for all vertebrae samples. | 92 |

List of Abbreviations

AALAS – American Association of Laboratory Animal Science
ALP – Alkaline Phosphatase
ANOVA – Analysis of variance
BATMAN – Batch Manager
BMC – Bone Marrow Cell
BMD – Bone mineral density
BNL – Brookhaven National Laboratory
BV/TV – Bone volume over total volume
CD – Control diet
cDNA – Complementary DNA
Conn.D – Connectivity Density
DHLA – Dihydrolipoic acid
DNA – Deoxyribonucleic acid
DP – Dried plum
FOS - Fructooligosaccharide
Gy – Gray (unit of)
H&E – Hematoxylin and Eosin
IACUC – Institutional Animal Care and Use Committee
IR – Ionizing Radiation
ISS – International Space Station
LET – Linear energy transfer
LPS - Lipopolysaccharide
MDA - Malondialdehyde
microCT – Micro Computed Tomography
min - Minute
NASA – National Aeronautics and Space Administration
AOX – Antioxidant diet cocktail
ORX – Orchidectomy
OVX – Ovariectomized
PBS – Phosphate-buffered saline
qPCR – Quantitative Polymerase Chain Reaction
RIN – RNA Integrity Number
RNA – Ribonucleic Acid
ROS – Reactive oxygen species
SMI – Structure model index
Tb.N – Trabecular number
Tb.Sp – trabecular separation
Tb.Th – Trabecular thickness
TBARS – Thiobarbituric acid reactive substance

1. Introduction

1.1 Background and Motivation

Astronauts are increasingly undertaking extended space missions. With advancing technology and the desire to explore the unexplored, astronauts may be in outer space for longer periods of time than before. Because of this, it is useful to understand how radiation in space affects bone health, resulting in bone loss. It is also beneficial to study potential dietary countermeasures that may influence osteoblast or osteoclast activity and determine how effectively they can protect from bone loss and promote bone formation. Research of this nature is also relevant to cancer patients undergoing radiotherapy, patients with osteoporosis, and postmenopausal women. It is known that osteoclasts have the primary role in bone resorption, as these macrophage-derived cells are known for breaking down bone during remodeling. It is also known that in space, both radiation and microgravity can lead to bone loss due to tissue damage and increased osteoclast activity. Most of the current treatments or supplements are limited because they only address bone resorption, not bone formation, or are otherwise too expensive or inadequate for the long term. For example, commonly used bisphosphonates are limited because they only reduce bone resorption rather than promote bone formation and the side effects include gastrointestinal discomfort, dizziness, and osteonecrosis in the jaw among others [8]. To this end, we are driven to continue research that is aimed at promoting bone health by studying the microarchitecture of irradiated bone and analyzing the gene expression primarily of bone markers in order to try to understand relevant molecular mechanisms of bone loss and formation. We additionally plan on analyzing potential protective effects of dried plum to determine its efficiency in mitigating bone damage from radiation. We envision that any findings will shed light on mechanisms involved in bone loss and/or formation.

The experiments conducted in this project are part of a more extensive study analyzing dried plum. At the time of these experiments, tissue samples had already been collected from mice (Figure 1). The project goals include bone and bone marrow cell analysis, gene expression, and microarchitecture analysis. Ultimately, the findings here should help advance the understanding of the mechanisms by which dried plum protects bone from the negative effects of radiation.

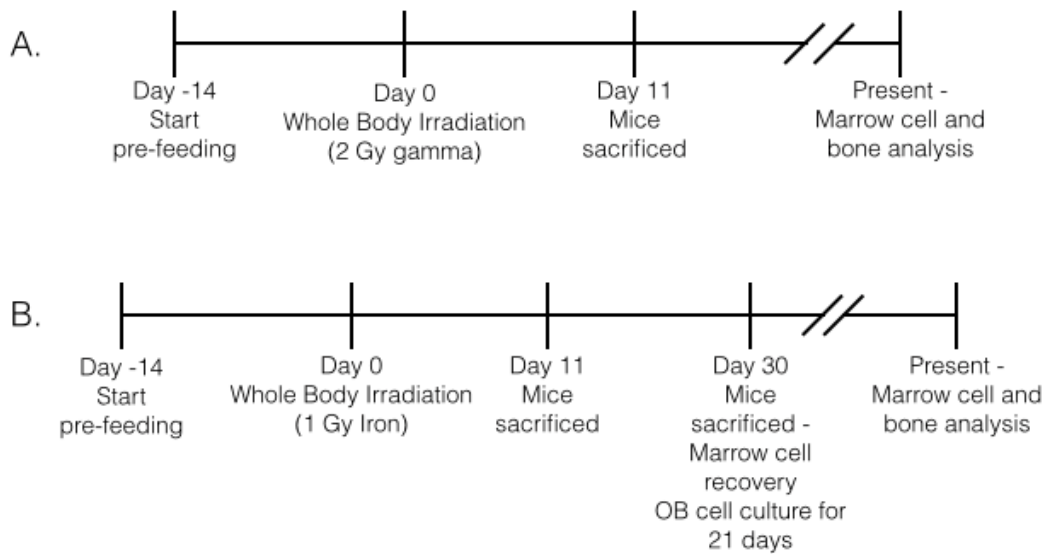


Figure 1. Timeline of experiments. A and B denote two different experimental set ups from which we will be analyzing samples. Two slashes indicate point at which our experimental design began.

1.2 Relevant Literature Review

1.2.1 Harmful Effects of Ionizing Radiation

Ionizing radiation's (IR) harmful effects have long been studied and findings have been presented in many ways to the common news consumer. Ionizing radiation is particularly harmful due to its ability to disrupt molecular interactions in tissues and organs. This occurs when radioactive atoms remove electrons from target atoms thereby altering its stability and molecular bonds. Moreover, ionizing radiation can induce DNA damage, including DNA double stranded breaks of the affected cells. Excessive numbers of double stranded breaks can overwhelm the DNA damage repair machinery, resulting in inadequate repair of the damage. The result will be mutations that are propagated during mitosis and, depending on the mutation combinations in question, cancer can result. Moreover, ionizing radiation can react with water within a tissue and cells to produce reactive oxygen species (ROS), which are reactive molecules that contain oxygen and can destabilize proteins and damage cell membranes [1]. Increased exposure to such radiation can lead to compounded damage, which raises concerns for the health of astronauts. Moreover, as Willey et al. points out, there is also a serious concern about astronauts' skeletal health besides the possibility of cancer, such as osteoporosis [2]. This therefore necessitates a closer study of the effects of radiation on bone health.

1.2.2 Measuring Radiation

Willey et al. explains the general terminology to measure radiation in [2]. The Gray (Gy) is the international unit of measure that represents the absorbed dose of radiation (D) in energy per unit mass, specifically Joules/kg [2]. But not all radiation is equal; for example, gamma radiation can be expected to differ in energy when compared to X-rays. Hence, Q is the symbol used to represent the quality of radiation and H represents the absorbed dose equivalent to yield the relationship that $H = D * Q$. For reference, the level of radiation to which cancer patients are exposed during radiation therapy for a gynecological tumor is about 54 Gy over six weeks, localized to the tumor [2]. In contrast, an astronaut may be exposed to up to 1-2 Gy of total body irradiation on an extended space mission outside low-earth orbit over a few years [3]. It is important to note that though the dose is lower in quantity, the difference between the two numbers above is that the astronaut receives full-body irradiation (as opposed to localized to a specific tissue) and the space radiation environment can be more damaging than the typical radiotherapy session, which often and mainly is composed of gamma rays and x-rays.

1.2.3 Space Radiation Environment

In order to allow for astronauts to embark on extended space missions, it is critical to first study the adverse conditions of space, particularly radiation, and to explore the viability of safety countermeasures to ensure the good health of space explorers. The space environment can be particularly dangerous to astronauts. Even though their vehicles have shielding to protect when inside, leaving the vehicle can expose astronauts to higher levels of radiation, especially during solar particle events. Solar particle events (SPE), otherwise known as solar flares, and galactic cosmic radiation are major sources of radiation in space. Galactic cosmic radiation is composed of protons and to a lesser extent of other ions that are “heavier than helium” such as iron; but in general all these particles are regarded as having a high charge (Z) as well as energy (E) [2]. The high-energy particles found in space can be referred to as high (H) charge (Z) and energy (E) particles, or HZE particles. Barcellos-Hoff et al. point out that radiation dose to which astronauts can be exposed depends on whether they are in the International Space Station (ISS), or on the surface of the moon or in deep space and furthermore adds that different tissues and cells within those tissues are affected differently depending on their relative position within the target organ or region [4].

1.2.4 The Skeletal System

The skeletal system is comprised of cartilage and bone as well as chondrocytes for cartilage production, osteoblasts for bone formation, and osteoclasts for bone resorption. During the development of the skeleton, a specific pattern - including the size, shape, and location - of bones is laid out often in large part by molecular cues, which lead to mesenchymal stem cells migrating and differentiating at the appropriate location [5]. Please refer to Figure 2.

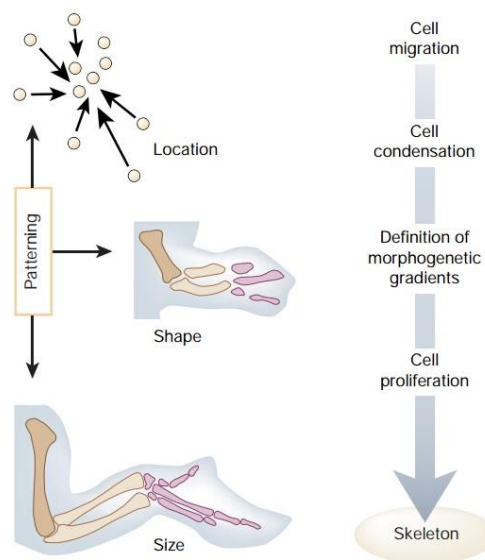


Figure 2. Skeletal development progression and patterning. [5]

Mesenchymal cells initially form a cartilaginous template that later becomes bone through the function of osteoblasts in a process called endochondral ossification. Experiments have shown that osteoblasts are able to effectively differentiate and proliferated in the designated areas set out by the initial developmental patterning event by the osteoblast gene expression in the target tissues; for example, the *Runx2* gene promotes osteoblast differentiation and high expression of this will induce osteoblasts to differentiate accordingly [5]. Though the knowledge of osteoblast and osteoclast differentiation pathways remains limited, it is evident that skeletal development and bone formation are complex processes. There are genes that promote bone formation and others that promote osteoclast function to resorb bone and molecular changes in these expressions are often the cause for certain degenerative diseases that affect bone mineralization, density, mass, strength, etc.

Throughout the general lifespan of a human, or any vertebrate organism, there is a frequent turnover of bone which is influenced by levels of use or disuse. It is important to recognize the distinction between the two types of bone tissue: cancellous and cortical. Cancellous, or trabecular bone, is usually found at the ends of bones (epiphysis) and contains vasculature to allow for blood and nutrient flow and other metabolic processes; furthermore, it is softer and more flexible. Cortical bone is the outer, hard layer of bone, which provides the mechanical strength and support. Both cancellous and cortical tissue can store and release calcium. Bone changes in response to physical stimulation or lack thereof. Experiments have shown that in response to loading, resorption occurs in the areas of the bone that receive low strain whereas bone forms where there is greater strains; moreover, axial compressive loading is a well-observed method to induce cortical bone formation [6]. This use/disuse bone remodeling aspect of bone physiology affects patients who undergo extended bed rest and the weightlessness that astronauts experience in space. The introduction of radiation into this system leads to an inflammatory response, which alters the delicate balance between osteoblasts and osteoclasts and as a result radiation leads to a net increase in osteoclast activity and therefore net increase in bone resorption, which leads to weaker bones. Cancellous bone is more sensitive to radiation and usually experiences most of the radiation-induced bone loss.

1.2.5 Characteristics and Functions of Osteoblasts & Osteoclasts

Osteoblasts always function as groups of connected cells and are responsible for bone formation. Osteoblasts that do not die become entrapped inside their collagenous-mineralized matrices, and then are considered to be more mature and termed osteocytes. In contrast, osteoclasts are responsible for bone resorption. They break down bone by secreting acid and collagenases often in areas of disuse. Both osteoblasts and osteocytes are derived from mesenchymal stem cells, which reside in the bone marrow near hematopoietic stem cell niches [19]. Osteoclasts arise from the differentiation of macrophages, which occurs when they encounter bone-like microenvironments produced by bone marrow stromal cells [20]. Osteoblasts and osteoclasts coexist simultaneously around the bone tissue but issues typically arise when the balance of osteoblast to osteoclast activity is altered.

1.2.6 Radiation Damage to Bone & Oxidative Stress

Radiation negatively impacts bone health, primarily by inducing an inflammatory response and oxidative stress, which triggers an upregulation of osteoclastic activity while suppressing osteoblasts. As a result, there is a net increase in the function of osteoclasts.

Nishio et al. evaluated the effects of certain treatments for endometrial, cervical, or ovarian cancer: platinum-based chemotherapy or chemo-radiation therapy, to determine what type of effect such procedures had on bone mineral density [12]. They found that the ovarian cancer and endometrial cancer groups showed slightly lower lumbar spine bone mineral density (BMD) while the cervical cancer group showed a significant decrease in lumbar spine BMD after surgery. This research has a different health application but still demonstrates the negative effects that radiation can have on bone mineral density in people.

Willey et al. note that bone loss occurs quickly in response to exposure to gamma or proton ionizing radiation, as observed in Figure 3 in which female C57BL/6 mice were exposed to either 2 Gy of whole body gamma or 2 Gy of proton radiation [2]. The authors further state that exposure to radiation decreases bone strength, increases fracture risk and decreases bone mineral density due to damage to the osteoblasts and osteocytes.

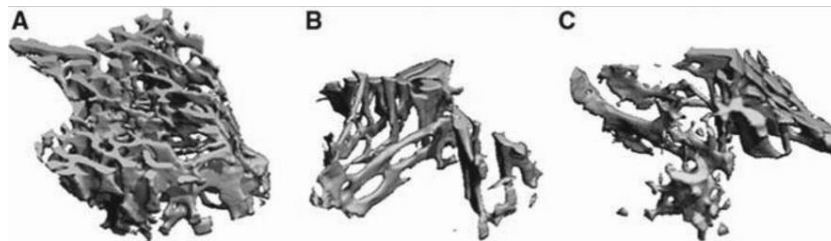


Figure 3. MicroCT images of trabecular bone. (A) Non-irradiated bone, (B) 2Gy gamma - whole body, (C) 2Gy proton radiation. [2]

Radiation damage that leads to rapid bone loss is mainly caused by increased bone resorption, a process, which is mediated by osteoclasts. Kondo et al. observed notable responses of bone loss: there was a decrease in both tibia and vertebra BV/TV, increase in osteoclasts normalized to the bone surface, and a reduction in mineral apposition rate (decrease in osteoblast activity) [3].

Lipid peroxidation is a process in which lipid moieties are oxidized; free radicals remove electrons from the cell membrane, thereby damaging the cell membrane. Kondo et al. measured lipid peroxidation by measuring the levels of malondialdehyde (MDA) and 4-hydroxynonenal levels, which are some of the end products of the process. They found that 2 Gy irradiation

increased lipid peroxidation after three days of exposure but no effect was presented from hindlimb unloading (Figure 4) [3]. Radiation leads to oxidative stress, which leads to damage in the bone tissue. These results suggest that potential dietary countermeasures with antioxidant properties may be able to mitigate radiation-induced bone loss. Many plants and fruits contain antioxidants that prevent reactive oxygen species from damaging cells and tissues, please refer to section 1.2.9 for more details.

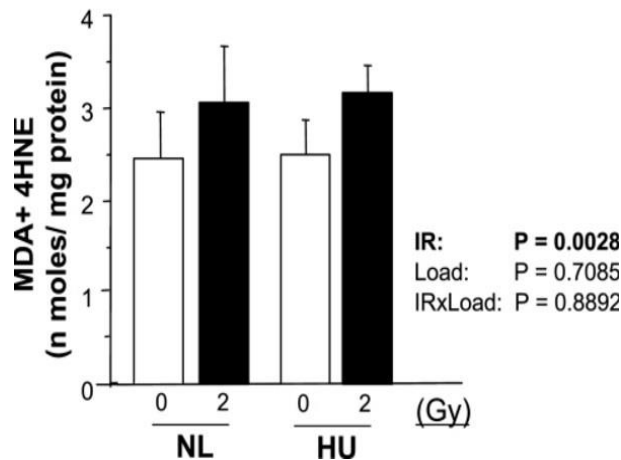


Figure 4. Radiation and hindlimb unloading effects on lipid peroxidation. [3]

1.2.7 Protective Effects of Dried Plum on the Skeleton

There has been an understanding that gonadal hormones contribute to skeletal health, and that the absence or change of hormonal makeup leads to skeletal deterioration. Franklin et al. tested this concept in combination with a dried plum diet with four groups of orchidectomized rats to determine the effects it would have on bone health [7]. This research demonstrated that even though orchidectomy (ORX) reduced the BMD of femurs and vertebra of these rats, a high dose of dried plum was able to restore BMD to levels similar to the sham group (Figure 5). Moreover, Franklin et al. showed that ORX decreased both the trabecular bone volume (BV/TV), as well as trabecular number (Tb.N) in the femur and vertebra, while increasing the trabecular separation (Tb.Sp) in the femur. Though there was no change in trabecular thickness due to ORX, every other physical characteristic was ameliorated by a high content of dried plum diet. This research

is significant because it presents dried plum as a viable supplement to promote bone health in the mouse osteoporosis model.

Similar to the experiment above, Rendina et al. conducted an experiment to test the effects of dried plum, apple, apricot, grape, or mango on the whole body and spine BMD in several groups of ovariectomized (OVX) mice [8].

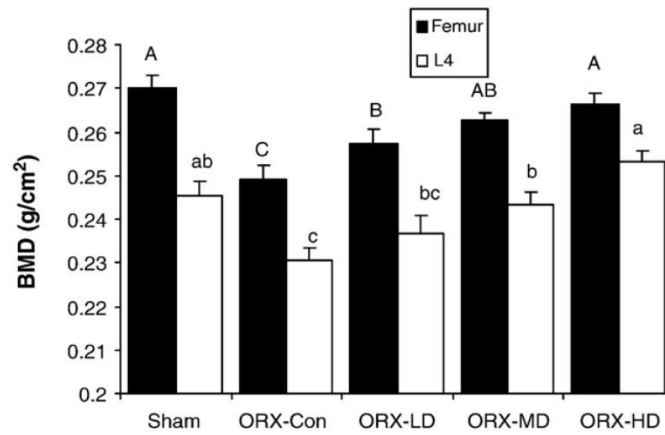


Figure 5. BMD results of dried plum acting on the effects of orchidectomy (ORX). [7]

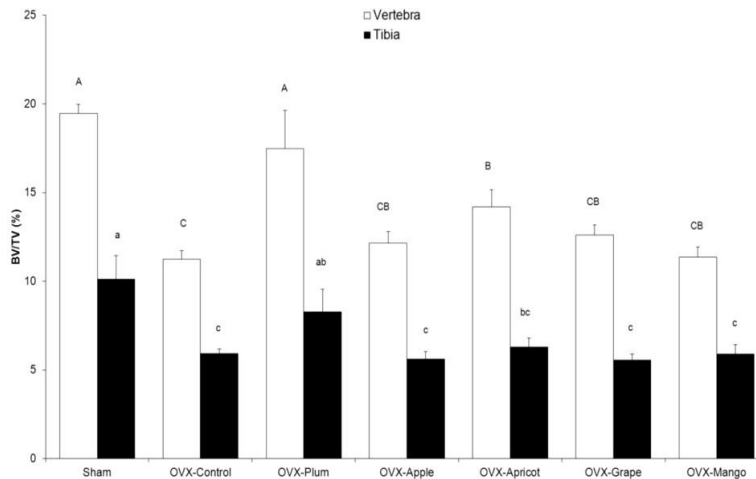


Figure 6. Changes in BV/TV of tibia in OVX mice in response to various dietary supplements. [8]

These experiments showed that the OVX procedure reduced whole body and spine BMD two weeks after the surgery, but after eight weeks of dietary treatment, the dried plum, apricot, and grape mouse groups had a higher whole body and spine BMD. Furthermore, OVX mice on the control diet underwent a 40% loss of trabecular bone in the vertebra and tibia; of the diet treatment groups, only the dried plum and apricot groups showed a higher vertebral BV/TV and

Tb.N (Figure 6). Rendina et al. used finite element analysis to study the mechanical properties of trabecular bone of vertebra of the OVX mice and sham mice and found a decrease in total force and stiffness in the bone of OVX mice, as compared to the sham group. This research once more underscores a relationship between gonadal hormones and bone health as well as the regenerative effects of certain fruits.

In a separate study, Schreurs et al. evaluated several antioxidant or anti-inflammatory interventions, including dried plum, for their ability to reduce bone resorption and prevent bone loss. The following interventions were tested in mice: (1) antioxidant diet cocktail (AOX) consisting of ascorbic acid, N-acetyl cysteine, L-selenomethionine, dihydrolipoic acid, and vitamin E; (2) dihydrolipoic acid (DHLA); (3) ibuprofen; and (4) dried plum (DP), 25% w/v. They studied the bone marrow one day after the exposure to either 2 Gy gamma radiation or 1 Gy proton/heavy ion exposure and found that genes related to bone resorption (osteoclast activity), such as *Rankl* and *Mcp1*, were upregulated as well as genes associated with the inflammatory response, such as *Tnf- α* . Schreurs et al. concluded that the most effective intervention was the dried plum-based diet [11].

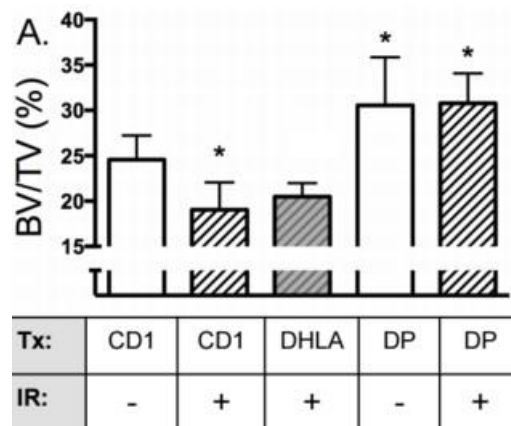


Figure 7. Dried Plum prevents bone loss induced by radiation. IR refers to proton and iron radiation, CD1 is the control diet.

However, in the presence of dried plum, the expression levels of the aforementioned genes returned to control levels. Schreurs et al. further note that while radiation led to a 32% decrease in BV/TV (Figure 7), 25% decrease in Tb.N, 13% increase in Tb.Sp in mice of the control group, mice with the dried plum diet did not exhibit any of the above structural changes [11]. Lastly, they observed that neither the AOX diet, ibuprofen, nor the DHLA diet prevented the radiation-induced bone loss. Therefore, radiation led to significant bone alterations, which the dried plum

effectively prevented. This raises two questions that we aimed to address in our project. Firstly, how does dried plum protect bone from radiation damage? Secondly, does dried plum enhance any bone regeneration/osteoblastic response? Dried plum has shown promising capabilities to restore bone health, but further analysis is required.

1.2.8 Effects of Dried Plum Diet on Osteoblast & Osteoclast Gene Expression

The bone-protective and regenerative effects conferred by dried plum have been observed over the past decade. The previously described study has shown that dried plum, in sufficient amounts, can reverse the damaging effects of radiation-induced bone damage. Though dried plum seems effective and promising for bone-related problems, about fifty grams of daily dried plum consumption is required to observe increases in bone mineral density [24]. This may be an impractical diet for astronauts to consume in space. The first step is to analyze gene expression for osteoclast or osteoblast-related genes and proteins in relation to dried plum consumption.

Phenolic acids are derived from the polyphenols found naturally in many fruits and vegetables. Polyphenols are suspected of being the driving force behind the bone protective

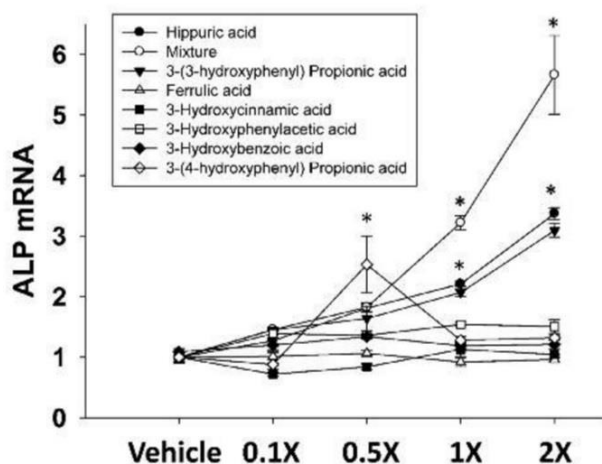


Figure 8. Effect on varying phenolic acids on ALP expression from rat serum. [11]

effects seen by dried plum. Chen et al. conducted a study to analyze the effects of phenolic acids on bone formation gene expression [12]. In this research, they found that when hippuric acid, propionic acid, or the phenolic acid mixture was added to a bone marrow ST2 stromal cell line, it led to an upregulation of alkaline phosphatase (ALP) expression, which is responsible for osteoblast differentiation (Figure 8). In addition to stimulating osteoblast cells, hippuric acid and

the phenolic acid mixture also inhibited adipocyte differentiation, as observed by cell culture proliferation assays of 3T3-L1 cells, which are pre-adipocytes. Though the results from this research are extensive and beyond the scope of this paper, it is important to note that when female mice were administered hippuric acid, they underwent significant trabecular bone accumulation and trabecular bone volume, and serum ALP levels were elevated too. Therefore the promising results shown by phenolic acids are observed both in cultured cells and in mice.

In a different study, researchers observed the effect of dried plum polyphenols on osteoblast activity and mineralized nodule formation. In brief, Bu et al. found that the three doses (5, 10, and 20 $\mu\text{g/ml}$) of polyphenols increased intracellular activity of alkaline phosphatase and promoted mineralized nodule formation [13]. *TNF- α* , tumor necrosis factor alpha, which is an inflammatory cytokine, decreased the expression of prominent bone formation markers such as *Osterix* and *Runx2*. However, polyphenols reversed this effect and also upregulated the *IGF-1* growth factor while suppressing the expression of *Rankl*. Rankl is the receptor activator of nuclear factor kappa-B ligand, which is a key factor involved in osteoclast differentiation. These findings lend credence to the observation that the inflammatory response (which can result from radiation among other factors) plays a key role in downregulating osteoblast-related factors while simultaneously upregulating osteoclast function. As before however, dried plum polyphenol extracts were able to attenuate these observed effects. These results suggest that either the polyphenol extract or a specific compound within the polyphenols promotes osteoblast function, very likely through antioxidant properties.

To complement the aforementioned findings, Bu et al. conducted a subsequent study to examine the effects on dried plum polyphenols specifically on osteoclasts and related factors, this time using lipopolysaccharide (LPS) to induce inflammatory conditions [14]. They measured production levels of nitric oxide (NO), a free radical, in RAW 264.7 macrophages as well as levels of *TNF- α* , and found both of these to be suppressed by the addition of polyphenols. *NFATc1* is a gene whose protein product can regulate expression of cytokines during the inflammatory response and induces osteoclast differentiation. In [14], Bu et al. found that dried plum polyphenols downregulated *NFATc1* in order to decrease the activity of osteoclasts and inhibit the differentiation of osteoclasts. Primary cell culture from C57BL/6 male mice's bone marrow cells were compared to RAW 264.7 macrophage cell cultures, and results indicated that dried plum polyphenols successfully inhibited osteoclast differentiation. In addition, their results

suggest that inflammation could be a source of bone loss and that dried plum appears to inhibit osteoclast proliferation.

Hooshmand et al. studied the anti-inflammatory and antioxidative qualities of dried plum polyphenols on RAW 264.7 cells [15]. They used lipopolysaccharide to produce inflammatory conditions and found that this inflammatory induction did not affect the viability of the macrophages. However, dried plum polyphenols reduced the nitric oxide levels that had significantly increased due to the LPS treatment and significantly reduced the levels of COX-2 protein, which is a prominent protein during the inflammatory response that produces prostaglandins. Inhibition of COX tends to alleviate symptoms of inflammation and pain and thus the dried plum polyphenols were able to attenuate the inflammation.

1.2.9 Other Natural Compounds

Fruits and vegetables (and the compounds contained within them) are widely known to contain many valuable nutrients essential to one's health, though only more recently have their association with bone been examined. While there has been research into the protective effects from other natural compounds, dried plum has been one of the most extensively studied. Dried plums, unlike many other fruits, have a characteristically high polyphenolic compound content apart from vitamin K, potassium, and boron [7].

In their comprehensive review, Sacco et al. postulate that despite the importance of calcium and vitamin D to bone health, there may be important factors like phytonutrients that contribute to healthy bones: lycopene, tea and grape flavanols, citrus flavanones, and olive polyphenols [16]. Lycopene is a carotenoid responsible for the red color of fruits like tomatoes and vegetables like carrots and is known to be a strong antioxidant. They point to a study in which lycopene was associated with an increase in BMD and a decreased risk for hip fractures. Rodent trials have also shown lycopene's protective effects against bone loss due to ovariectomy. Flavanols, the most common of which are catechin and epicatechin, are found in red wine, green tea, and grapes. The authors cite epidemiological studies that draw a connection between "habitual tea drinkers" and higher BMD and continue by pointing out that consumption of green tea leads to a higher serum level of alkaline phosphatase, which is a known osteoblastic marker [16]. Also, grape seed proanthocyanidins were shown to increase bone formation in developing rats [17]. Hesperidin is a major citrus flavanone found in oranges and has been

shown to protect against bone loss that arises in postmenopausal women [17]. Moreover, it has been shown to improve bone mass in rats and prevent bone-loss due to ovariectomy. Oleuropein is a major polyphenol found in olives and consumption of Mediterranean diets (with high contents of olive oil) were associated with increased bone mass. Though concrete evidence of such effects are still missing, preliminary investigations with developing rats have shown promising results with oleuropein's ability to protect or enhance bone mass [16]. Sacco et al. lastly cover dried plum polyphenols and point to its many beneficial effects as seen in preclinical as well as animal studies: increase in bone formation markers including *ALP* and *IGF-1*, increase in BMD at the spine and ulna, increase in bone marrow myeloid and lymphoid populations to suppress the immunological responses from ovariectomy, and increase in bone mass and bone strength.

In a rat study, Johnson et al. found that fructooligosaccharides (FOS) in combination with dried plum was able to protect against bone loss and promote bone formation most successfully, in comparison to a soy protein-based diet, FOS alone, or dried plum alone [18]. FOS is a prebiotic and oligosaccharide composed of fructose unit chains, which is found in onions, garlic, bananas, artichoke and other plants. While FOS and DP on their own were able to promote femoral BMD, Tb.Th, Tb.Sp, and bone mineralization as well as a lower urinary *Dpd* expression (marker for bone resorption), the greatest benefit was seen with the combination of all components in the diet. This suggests that FOS has a particularly ameliorative effect on the skeletal system. As Johnson et al. point out, FOS promotes the absorption of minerals from the colon and increases bone mineralization [18]. Generally, the effects of dried plum on BMD, BV/TV, Tb.Th, Tb.N, and Tb.Sp more or less equaled those of FOS. This may be because this study only utilized a 7.5% w/v dried plum in experimental diets whereas other similar studies previously alluded to use considerably higher dried plum levels (up to 25%, as in [11]). However, it is difficult to undertake accurate comparisons since no study has compared a 25% dried plum diet with any level of FOS.

Numerous other natural compounds were mentioned in this section, all displaying some level of antioxidant and/or anti-inflammatory and/or bone protecting effects. To our knowledge there has been no comprehensive study aimed at comparing all these individual compounds against each other so it is not entirely plausible to rule out any of them completely due to a lack of bone protection capabilities. However, scientists have shown that dried plum-based diets

demonstrate positive bone effects in rat and mouse models [7-8, 11]. Promising results have also been observed in humans [24]. In any case, we have chosen to continue studying the effects of dried plum in this research project, acknowledging that even though other compounds may also confer valuable skeletal health boons, dried plum is the only dietary supplement shown to mitigate radiation damage in bone. Also, our time and funding is limited and so it is also impractical to attempt to expand beyond dried plum.

1.3 Current Therapies

In order to prevent the risk of fracture caused by loss of bone strength due to extended missions on the International Space Station (ISS) and possibly Mars, astronauts are required to follow a strict, daily exercise regimen. Exercise alone is not sufficient to overcome the increase in bone resorption as well as the decrease in bone formation. Maintenance of bone homeostasis is crucial to the prevention of osteoporosis development in astronauts as well as in clinical osteoporosis patients. Bisphosphonates have held a clinical role in the treatment of osteoporosis for approximately 3 decades [9]. This therapy has been shown to inhibit the activity of osteoclasts in the bone. This inhibition is achieved primarily by advancing the apoptosis of these bone-degrading cells. As a result, bisphosphonate has been prescribed to astronauts to mitigate bone loss. Therapeutic intervention with the administration of bisphosphonates has presented the possibility of several adverse side effects [10]. Short-term side effects include severe musculoskeletal pain, hypocalcemia if patient consumes inadequate amount of Calcium and Vitamin D, ocular inflammation, and long-term side effects include over-suppression of bone turnover and sub-trochanteric femoral fracture. These side effects remain to be a rarity, but the complication risks merit analysis of treatments that eliminate the possibility of these side effects. Dietary supplements of Calcium and Vitamin D have also been studied and have become part of the regiment of therapies for astronauts to protect against bone fracture [11]. The necessity to examine alternative therapies is due to the fact that all but one current therapy are anti-resorptive, but do not promote bone formation; alternative therapies are also necessary due to the possibility of adverse effects of bisphosphonate therapy.

1.4 Project Goals and Experimental Design

Previously, four groups of mice were pre-fed and acclimatized to their laboratory environments for two weeks at which time they were irradiated with 2 Gy of gamma radiation and the first three groups of mice were euthanized (Day 0). Three more groups were sacrificed 11 days post irradiation. Another four groups of mice underwent the same experiment as just stated in the previous sentence, but were irradiated with 1 Gy iron radiation.

Our research aims are to (1) determine the molecular responses of bone to radiation and evaluate the efficacy of a dietary countermeasure against bone loss caused by radiation and the underlying mechanisms for its protective effects, and (2) determine the ability of dried plum to protect the axial skeleton (vertebrae) from ionizing radiation. There are various options to mimic solar particle events and galactic cosmic radiation, which astronauts are exposed to during space travel. These include exposure to high and low linear energy transfer (LET) radiation. Gamma radiation (low LET) and Iron radiation (high LET) is thought to be a viable representation of actual radiation doses in outer space [2-3, 11]. Thus, irradiation of mice with gamma radiation and another study with Iron (^{56}Fe) radiation was utilized to accomplish our research goals. Our experimental design will also include gene expression via Quantitative Polymerase Chain Reaction (qPCR), oxidative damage measurements, and micro-computed tomography (microCT).

The dietary supplement in question has shown promise in bone remodeling, but has only recently been evaluated for its radio-protective effects [11]. Current treatment options only inhibit the activity of osteoclasts, as stated in the previous section, but our research aims to determine whether the dietary supplement in question in conjunction protects the progenitors and stem cells that differentiate into mature, bone forming osteoblasts, apart from its previously known ability to inhibit osteoclast activity. Thus, our project focuses on the hypothesis that the mechanism by which the dietary supplement acts to protect bone against effects of space radiation has the potential to be both anabolic (increasing the mechanistic cues for bone formation) as well as inhibiting osteoclast formation.

1.5 Significance

A journey to Mars and the future of long-term space travel depends heavily on knowledge and interventions surrounding the bone loss caused by the radiation present in the space environment.

These health concerns caused by radiation are not limited to astronauts, but extend to radiotherapy patients as well. The increase in bone loss seen in postmenopausal women and individuals suffering from osteoporosis is similar to the bone loss resulting from clinical and space environment radiation [2-3, 11]. Thus, our research may provide a better understanding of bone loss in these conditions. By analyzing the nature of osteoblast and osteoclast expression in response to radiation and attempting to reduce viable molecular mechanisms by which they are up or down regulated, we hope to advance current knowledge that may later help improve current treatments or methods for promoting bone health.

1.6 Team and Management

The success of this research project relied on the cohesive and enthusiastic nature of our team. Success was determined based on our involvement and team management collaboration with the larger Bone and Signaling Laboratory at NASA Ames Research Center. Our research was part of a greater experiment directed by our advisors, Dr. Ann-Sofie Schreurs, Dr. Candice Tahimic, and Dr. Ruth Globus. Dr. Prashanth Asuri served as our advisor through the Bioengineering Department at Santa Clara University.

Regular meetings with Dr. Schreurs ensured that the project remained on schedule and that design problems or experimental deviations were discussed immediately. Bi-weekly meetings with Dr. Asuri were held to make certain that project process was being made and all thesis deadlines were met.

1.6.1 Budget

This senior design thesis project is funded by NASA grants. Please refer to Appendix A for a breakdown of estimated costs for this project.

1.6.2 Timeline

This senior thesis project progressed throughout the entirety of the 2015-2016 academic year. During our fall quarter we completed all necessary safety training in order to take part in functional laboratory protocols. This included, but was not limited to, animal safety training, biohazard safety training, radiation training, and general lab safety standard operating procedures. By the end of the fall quarter we also studied and reviewed a significant portion of

the applicable academic literature on our thesis topic and began training for lab-specific procedures.

During winter quarter we delved more extensively into laboratory procedures related to gene expression analysis and oxidative damage analysis.

Throughout our spring quarter we focused on micro-computed tomography (microCT) and finalized any necessary experiments while also determining future work that can and should be performed as a continuation to our experiments.

2. System Level Experimental Design

2.1 System Level Overview

Our literature research demonstrated several key observations, which we considered during the planning of our experimental approach. Ionizing radiation, which is prevalent in space and used during radiotherapy, induces DNA damage and causes increased generation of reactive oxygen species that lead to oxidative damage, ultimately resulting in tissue damage [1-4, 11]. Radiation-induced bone loss is largely attributed to bone resorption, which is mediated by enhanced osteoclast activity. Dried plum has been shown to mitigate radiation-induced bone loss [11]. It is believed that polyphenols contribute specifically to this protection against bone loss and that they primarily function by blocking bone resorption. Hence, the main focus of this research project is to determine the mechanism by which dried plum protects bone.

Like any hypothesis-driven research in an educational setting, our project has changed its focus and schedule several times due to necessary adjustments and challenges encountered from week to week. Nevertheless, we were able to follow a general outline of experiments that facilitated the collection of relevant data at the gene expression and mechanical testing levels. An overview of the experiments performed follows (Figure 9).

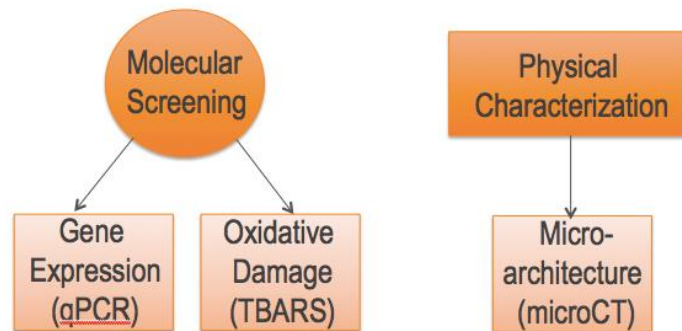


Figure 9. Overview of experiments we undertook for our senior design project. Our experimental design was divided into two phases: molecular screening and physical characterization.

The first major procedure was the extraction of RNA from bone. At the commencement of this project we had access to several tissues from the radiation/dried plum experiment. Because we aimed to study the role of dried plum in bone loss prevention, we opted to use the frozen left femurs and marrow collected from animal experiments predating our tenure in the lab. Femurs were utilized in order to extract the greatest amount of RNA as possible per bone; while

the tibiae and vertebrae were scanned by microCT to analyze bone micro-architecture and in continuation, the vertebrae will be utilized for mechanical testing. We needed to extract RNA for the eventual purification, preparation, and analysis of gene expression (of osteoclast, osteoblast, and oxidative stress related genes) by qPCR. Please refer to the Materials and Methods section of chapter 5 for a detailed description of the procedure.

An intermediate step required prior to gene expression analysis via qPCR is to first convert the extracted RNA to cDNA. This step involves the use of a reverse transcriptase to convert the single stranded RNA into its complementary DNA, which can then be used as a template for the qPCR procedure. Though it is possible to perform this as a one-step assay that combines reverse transcription with qPCR in the same reaction tube, we opted to take the time to complete a dedicated cDNA conversion step on its own, for several reasons. Firstly, doing a two-step procedure allows us to optimize the reagents and master mixes used specifically for the previously extracted RNA. Afterwards, these cDNA samples can be stored frozen for subsequent use in further qPCR analysis. Because we aimed to test numerous genes at various times throughout our time in this lab, having a store of cDNA was favorable. Our lab has also demonstrated that a more careful, two-step cDNA synthesis procedure leads to more reliable results. Please refer to the Materials and Methods section of chapter 6 for a detailed description of the procedure.

The qPCR was conducted as follows: cDNA samples were first prepared from the original RNA samples through reverse transcription. Ultimately, qPCR was performed and the gene expression data analyzed. In brief, the genes we tested either in bone (flushed, devoid of marrow) or bone marrow cells are the following: *Bglap*, *Foxo3*, *Nrf2*, *Postn*, *Sost*, *MTOR*, *Cdkn1a*, *Gadd45a*, *p53*, *BMP2*, *BMP4*, *Rankl*, *Opg*, *Runx2*, and *IGF-1*. Please refer to Appendix I for a detailed description of the genes that we observed.

Extensive gene expression analysis of this nature would potentially allow us to draw connections or observe correlations between osteoclast and osteoblast-related genes, the exposure to sham or ionizing radiation, and whether dried plum contributed to its respective increase or decrease. If dried plum protects bone and stimulates its formation, we should expect to see an increased expression of bone formation markers and/or a decrease in bone resorption markers in the dried plum compared to control diet group.

Apart from gene expression, we also aimed to measure oxidative stress and damage. The rationale behind such experiments is that radiation leads to increased production of reactive oxygen species followed by oxidative damage that can be measured via the malondialdehyde (MDA) quantification assay. It is known that MDA is a result of the oxidative stress response, and is one of the oxidative damage markers. A higher level of this organic compound can be attributed to a greater level of oxidative damage. Therefore, by measuring MDA levels in blood serum and bone samples we hoped to ascertain the extent that radiation increases MDA and dried plum reduces this same compound. To measure MDA levels, we used Thiobarbituric Acid Reactive Substances Assay (TBARS assay), which relies on the thiobarbituric acid compound reacting with MDA to produce a fluorometric response that can be measured at around 550nm wavelength with a plate reader.

The first step was to conduct an experiment to determine the adequate dilution concentrations of bone samples and serum samples such that readouts fall within the linear range of the assay. Doing this in conjunction with the microBCA assay to measure the total protein concentration present in all the samples, we could determine whether we had an adequate dilution or not. Depending on the sample type, we tested dilutions ranging from 1/50 to 1/10 (see Materials and Methods section of chapter 8 for details). The resulting data allowed us to conclude that further dilution experiments are required to obtain a more optimized dilution factor that is within the linear range for the TBARS assay. After the success of this dilution experiment, the actual TBARS assay was run on the available samples of bone and blood serum.

The abovementioned experiments focused on analyzing biochemical changes related to the extent of oxidative damage at the molecular level. While this information can provide insights into the mechanism by which dried plum protects bone, it is also of great benefit to analyze physical characteristics, namely bone micro-architecture (tibia and vertebrae) either in response to radiation or dried plum diet (trabecular number, trabecular thickness, bone volume per total volume, bone mineral density, etc.) as well as their mechanical properties, such as stiffness and compressive strength. Explanations of these terms and more details for this testing are provided in Chapter 9/Appendix K. The rationale behind analyzing the physical characteristics and mechanical properties is to better understand how dried plums affect bones at the molecular level as well as at the structural level. Mechanical testing can determine the

strength and elasticity of bone, and thus its quality. It complements the microCT results of mineralized structure.

At the beginning of our project we had planned to conduct an extensive *in vitro* experiment, but for several reasons priority was given to gene expression analyses, microCT scanning, and mechanical testing. The *in vitro* experiment would have involved MLO-Y4 cells (osteocyte cell line) and/or primary cell culture from bone marrow cells of mice. This experiment would have required the extraction and purification of polyphenols from the dried plum since the overall goal of this experiment is to determine the bioactive component in dried plums – and whether polyphenol(s), and in what combination, when applied to irradiated cells in culture, were the actual component responsible for bone protection and formation. Though the results from this experiment would have been incredibly interesting and a great complement to our overall results, we had limited time during this academic year and could only select a handful of experiments. The reason gene expression, TBARS, and microCT were prioritized is that these analyses result from *in vivo* experiments (MLO-Y4 is a transformed cell line). This allows us to study the direct effects that both radiation and dried plum had on mice bone and bone marrow cells, as well as determine the relevant pathways that play a role in bone loss and the protective affect of a dried plum, supplemented diet.

2.2 System Level Constraints

There are several constraints and limits to the research that we performed in the Bone and Signaling Lab. These constraints influenced the course of our experiment planning as well as experiment prioritization so that we could obtain viable results.

RNA extraction

The RNA extraction from bone procedure was labor-intensive and required several days of work and meticulous planning to ensure that all mouse left femur samples were properly processed. Each bone was homogenized with a handheld tissue homogenizer and was followed by Trizol-based RNA extraction. As the procedure involves a Trizol reagent (details in the respective Methods section, chapter 5) and we desired to separate the homogenized samples into different phases to obtain the RNA, DNA, and protein sections, careful handling was also required. All steps of the RNA extraction post homogenization were time sensitive and needed to be

completed as fast as possible in order to ensure the highest level of RNA integrity. The technical goal of the RNA extraction process was to generate RNA of acceptable concentration and “RNA integrity number” (RIN). RIN measurements were determined using an Agilent Bioanalyzer, a chip-based instrument. All samples met target concentrations and RIN values and so were used for cDNA conversion and subsequent qPCR.

Conversion to cDNA

The cDNA conversion procedure also presented some technical challenges. This assay required the use of a thermocycler at fluctuating temperatures for set time durations and the proper addition of specific master mixes and primers to allow the single stranded RNA's to be converted into the corresponding complementary DNA. We encountered problems during our initial attempts to produce good cDNA both in quality and in quantity (which we found out in the qPCR step when there were poor or erratic results in the gene expression). Though not indicative of actual cDNA quality, we still tested the sample concentrations in the Nanodrop to confirm that the cDNA conversion procedure yielded sufficient amounts afterwards (data not shown).

qPCR Analysis

If our initial hypothesis is correct, then radiation should decrease the expression of genes associated with bone formation or protection and/or upregulate the expression of genes involved with bone resorption and cell cycle arrest. A dried plum diet should therefore lead to an upregulation of the expression of genes associated with bone formation or decrease bone resorption. Please refer to our table of genes (Appendix I) for more information on the specific genes analyzed for each of these categories. However, our analysis is limited because the changes we hoped to observe may not be apparent at 11 days post-irradiation, the time point at which the mice were euthanized and their tissues collected for this experiment. It is possible that some of the gene expression changes occurred at an earlier time point, such as at 1 or 2 days post-irradiation. In this case, the tissue samples that we analyzed may not have shown the expected results. Further analyses are required to determine whether this is the case. A future experiment that could confirm this hypothesis is to test tissues that were collected at different time points, ranging from 24 hours post-irradiation to 11 days.

A limitation to our gene expression analysis was the low amount of RNA sample we had to work with. Due to a relatively low concentration of RNA we were able to extract, we could only obtain a limited amount of cDNA and thus only test a limited number of genes. The genes that we selected were prioritized on the basis of their general function, primarily those shown to be commonly involved in bone resorption, bone formation, oxidative stress, or cell cycle arrest, as well as on literature.

Oxidative Damage Analysis (TBARS assay)

One constraint of the analysis of oxidative damage by the TBARS assay is that there is a possibility that it is not 100% specific only to MDA. We are not positive if the assay is only measuring MDA/lipid peroxidation or if it is quantifying other compounds as well.

Micro Computed Tomography

The scanning of mouse vertebra is a time-consuming procedure, which limits the scanning to about four or five bones per day. Note that in total we had forty bones to process. This prevented us from undertaking a considerable portion of the actual mechanical testing.

Post-processing of the L4 vertebrae scans were also time-consuming. Initially we faced some challenges in setting the boundaries and volume of the L4 vertebrae to process. Due to inconsistencies from vertebra to vertebra, we had to test a variety of buffer region sizes and region of interest sizes in order to ensure all our vertebrae could be uniformly compared with one another. After extensive trial and error testing, we finally set the final region of interest to be 260 slices (these slices collectively form the volume of interest that we analyzed), with no buffer zone above the growth plate at the caudal region of the vertebral body.

2.3 Experimental Approach

The project we have described in this thesis is notable for several reasons. In terms of senior design projects conducted at Santa Clara University, ours is the only project of this nature: one involving the study of a specific diet in its role to prevent bone loss that is of relevance to astronauts, as well as to post-menopausal women and radiotherapy patients. Our project ultimately aims to elucidate relevant molecular pathways by which dried plum inhibits bone resorption, knowledge that could, in the future, be used to develop strategies to maintain the bone

health of astronauts during and after space missions. With this overarching NASA goal in mind, we diligently delved into extensive literature research, laboratory training, and established a solid experiment schedule throughout the quarter.

Literature research was the basis for the experiments performed, as it gave us the background to learn about the relevant bone physiology resulting from exposure to radiation as well as observed effects of dried plum. By studying literature extensively, we were able to identify relevant genes that we could test in our experiments, and thus identify any possible role that dried plum had in bone resorption and formation.

The nature of this type of research necessitated a flexible schedule and experimental plan, as each week's results often provided critical information, such as whether or not we were conducting the experiments properly, whether the results we obtained were reasonable and promising, whether the assays or experiments were suitable for what we were trying to solve, or whether our results were altogether irrelevant or uninformative in the grand scheme of our final goal: to determine the mechanism by which dried plum protects bone. As such, the priorities for what we hoped to do shifted on a week-by-week basis and it was necessary to adapt accordingly.

As with any lab-intensive research project, we encountered several challenges along the way. This necessitated the repetition, namely when we were performing the conversion of RNA into cDNA, of said experiments. Overall, it was a truly enriching experience to work in the lab environment in which we found ourselves. We were surrounded by incredible and highly knowledgeable scientists who provided invaluable direction every step of the way.

Though the research that we are working on is vast, we are confident that the results and accomplishments during our tenure in the lab are, on their own, solid contributions that will hopefully help promote a better understanding of the radio-protective effects of dried plum.

2.4 Engineering Standards and Realistic Constraints

Our research project in the Bone and Signaling lab is purely research-oriented that does not, at our stage in the lab, translate into any direct product for any consumer. What we hope to achieve is a greater understanding of the mechanism by which dried plum protects bone so that at some point in the near future, the active components or mechanism in question can be utilized to produce a treatment or supplement that will aid in bone health, especially, but not solely for astronauts. With this in mind, the final goal in mind is the bone health of astronauts as well as

patients with bone diseases. Thus, results from our research and future research with its accompanying results could have implications on the *health and safety* of astronauts as well as radiotherapy patients and individuals suffering from osteoporosis.

As such, health is a significant, albeit distant, aspect of our research. A realistic constraint in the use of dried plum for bone formation is that in order for dried plum to produce the desirable effects described in section 1.2 above, a very large amount of dried plum must be consumed on a daily basis. This is, of course, impractical for anyone seeking to improve his or her bone health or promote bone formation. This is precisely why we seek to study the actual mechanism at the molecular level, so that we may observe what molecular pathways dried plum acts on, and moreover to eventually identify the active component within dried plum responsible for the regenerative effects on bone and use that to develop a better treatment. Thus, this active component could potentially be concentrated into a supplement tablet consumable by astronauts or patients with bone diseases. This lends itself as a societal implication related to *manufacturability*. It would be easier to extract and manufacture a supplement tablet from a naturally growing fruit, i.e. plum, in comparison to synthetically manufacturing a drug to serve the same purpose in a pharmaceutical company.

An *ethical* consideration related to our specific project, though we did not directly work with this part, is the use of mice. Though animals in scientific research can potentially raise moral objections by some people, it is important to consider that in this case, the mice used in the preceding procedures for our research were handled humanely and according to the American Association for Laboratory Animal Science (AALAS) standards for handling of laboratory mice. Also, all animal experiments were conducted following a standard set of protocols and guidelines pre-approved by the Institutional Animal Care and Use Committee (IACUC). The mouse was a suitable model because much like the bone loss seen in astronauts due to spaceflight, mice also experience bone loss due to radiation and hindlimb unloading (used to mimic a microgravity environment). Mice are the most developed species for experimental procedures and are viable for research of this nature. Ten mice were needed per group (four groups) and the justification for this amount is that this is the number that will allow for statistically significant results once the data is analyzed, due to the high variability of microCT and other assays. It can be said that the use of mice in our experiment was justified and essential in order to promote and advance the

scientific understanding that will one day lead to more effective treatments for astronauts' bone health.

Other than what was mentioned above, there are no outstanding ethical concerns with the nature of the experiments we conducted, as we mostly worked at the molecular level, with tissues that had previously been collected. We mostly worked with RNA extractions, qPCR, and other molecular biology-based assays.

The future research prospect of this project also has *economic* implications. The overarching goal for this research, as stated above, is to extract the active components of dried plum and determine which components, either on their own or in a particular combination, serve to best protect bone against the damaging effects of radiation. The introductory work to determine the most effective active components can be performed through an *in vitro* cell culture experiment. *In vitro* experiments are much more cost effective than *in vivo* experiments. Thus, it is economically productive to first determine which active components are most effective *in vitro* and then confirm these successes and their efficacy in an *in vivo* experiment.

Though our project did not directly have any ethical implications, there are other considerations, should our research be expanded and developed into an actual consumer product (i.e. a dietary supplement) that people can take to better their bone health. Mainly, any product that arises from parts of this research must be safe and effective with the consumer; whatever the specific dried plum component that may be isolated must be formulated in such a way that it doesn't negatively affect the patient's health, but rather promotes it. But again, this stage of the research remains distant and is not an immediate consideration that we had.

3. Design Description

3.1 Design Overview

To reiterate the general points of chapter two, we performed the following experiments: RNA extraction from the left femurs of mice, conversion to cDNA in preparation for qPCR, qPCR gene expression analysis of osteoblast, osteoclast, or oxidative stress related genes, TBARS assay, and scanning and analysis of mouse vertebrae to observe the physical structure of bone, either in response to radiation and/or after dried plum treatments.

As stated above, these experiments were all necessary for our research. RNA extraction, followed by conversion to cDNA, allowed us a tangible, molecular entity to manipulate and work with from which we could analyze gene expression. qPCR was the method by which gene expression was measured and quantified and we ended up testing a number of genes of interest; please refer to Appendix I for the list of specific genes. TBARS required initial dilution experiments and when performed on samples helped provide an idea of the relative level of oxidative stress in different tissues from the designated sample groups. Lastly, observing the characteristics of bone from these mouse groups proved to be a useful complement, as it allowed us to observe the overall microarchitecture of the bones after radiation and dried plum diet consumption.

The nature of the experiments we performed throughout this yearlong senior design project belonged either to the category of gene expression, protein/oxidative stress assay, or microCT and mechanical testing.

QPCR was used for gene expression to study the levels of RNA transcribed from genes of interest and so provide information related to which genes are upregulated and expressed or downregulated in response to radiation or a dried plum diet.

Experiments or assays to gauge oxidative damage at the protein or lipid level are particularly useful because proteins do the actual work in just about every biological process. During oxidative stress, certain proteins may be activated or repressed, etc. Experiments in this category can include the already mentioned TBARS assay as well as other procedures such as Western blots or ELISA assays. The TBARS assay will detect MDA (oxidative damage marker) within the total protein level found in the samples tested.

Scanning with microCT and undertaking mechanical testing procedures would validate or support the results found at the gene and protein levels. We should expect to see the bones from irradiated mice to have a compromised structural integrity compared to the bones collected from the dried plum group, as well as the ability to analyze how radiation and/or dried plum can influence the structural integrity and other mechanical characteristics of bone. Said characteristics can include bone volume (BV/TV), trabecular thickness (Tb.Th), trabecular number (Tb.N), bone mineral density (BMD), etc. Mechanical testing can include three-point bend tests, axial compression tests, yield strength, and others. Each of these would allow us to see how irradiation or dried plum physically affects the structure and mechanical properties of axial and/or appendicular bones of mice.

The following is the outline of procedures we performed:

1. **Phase 1, part 1:** Gene Expression
 - a. RNA extraction from bone.
 - b. Conversion to cDNA.
 - c. qPCR to analyze specific genes of interest.
2. **Phase 1, part 2:** Oxidative Damage Analysis
 - a. TBARS assay, lipid based to analyze relative oxidative damage.
3. **Phase 2:** Physical Characterization
 - a. MicroCT Scans of Mouse Vertebra.
 - i. Vertebral scanning.
 - ii. Post-processing (i.e. reconstruction, rotating, contouring, analysis)
 - iii. Mechanical testing (i.e. strength tests)

The experiments outlined above were performed in the order listed because gene expression was a faster, molecular biology-based experimental technique that we could perform more efficiently in the beginning of our time in the lab. From gene expression analysis we could easily obtain valuable information on the effects of radiation and dried plum diets at the molecular level. Results of the qPCR, specifically genes related to oxidative stress, were complemented and enhanced by the TBARS analysis of oxidative damage. TBARS assay was performed because it allowed us to study the effects of radiation and dried plum at the protein/lipid level. MicroCT provided us with information about the micro-architecture and bone mineral density of the L4 vertebrae. Mechanical testing, which takes the longest time (in terms of

training and execution), was left for the end. This provided valuable information about the structure and strength of bones in response to different treatments (radiation, dried plum, control). Mechanical testing was prioritized towards the end due to the possibility that the gene expression analysis may not be a wholly accurate indicator of the efficacy of dried plum diet as the tissues were collected relatively late, at 11 days post-irradiation. By studying changes in the mechanical properties, we could determine whether our gene expression experiments show any correlation with the bone microarchitecture.

3.2 Expected Results

The expectations for each facet of our research project are outlined below. These expectations are based largely on extensive literature research.

For our first phase, we expected to extract RNA in high enough quality that our samples yielded a RIN number between 9 and 10. For the RNA Nanodrop concentration verification, we hoped to have a high RNA yield after homogenization of bone samples; if RNA quantities were high we would dilute them all to 100-150ng/uL.

For the actual gene expression, we expected radiation to increase or upregulate many genes associated with bone resorption (*Rankl*, *Opg*, *Sost*, and *Nfatc1*) and oxidative stress or cell cycle arrest (*Nfe2l2*, *Foxo3*, *Cdkn1a*, *Tp53*, *Gadd45a*, *MTor*, and *Sod1*). This is because radiation is known to damage biological tissues through the production of reactive oxygen species, resulting in oxidative and DNA damage, among other injuries; cell cycle arrest occurs as a protective response to radiation. In samples from mice that received the dried plum treatment, we would also expect these same values to be reduced or remain unchanged, relative to the controls. We also expected that the genes associated with bone formation (*Runx2*, *Bmp4*, *Igf-1*, and *Bmp2*) would be upregulated in the samples that belonged to the dried plum diet group. An increase in osteoblast-related genes would signify that dried plum acts not only to inhibit bone resorption, but also to promote bone formation.

For the TBARS protein oxidative stress analysis, we hypothesized that samples from mice that were exposed solely to radiation and fed the control diet will exhibit a higher level of MDA. We also hypothesized that samples whose respective groups received the dried plum diets will exhibit lower (or baseline level, similar to control) MDA levels.

For microCT scanning of mice L4 vertebra, we expect that samples derived from the mouse group that received the dried plum diet will show a microarchitecture with higher BV/TV, higher Tb.N, and overall structure with greater physical integrity. On the other hand, samples from mice that were exposed to radiation would exhibit lower BV/TV and Tb.N.

4. Historical System Setup

4.1 Introduction

Prior to the time that we joined the Bone and Signaling laboratory, the experiments discussed below had been completed, but tissue analysis had not been conducted yet. In order to understand the experimental protocols we conducted throughout this yearlong thesis project, the historical experimental set up needs to be introduced. Two experiments will be presented. Both experiments were designed to investigate the protective effect of dried plum on bone after exposure to ionizing radiation, but the species of radiation is the differing variable between the two experiments: (1) mice were irradiated with 2Gy Gamma radiation and (2) mice were irradiated with 1Gy Iron (^{56}Fe) radiation. Although gamma and Iron are notably two different types of radiation, they are representative of different types of whole body radiation experienced by astronauts in the space flight environment. They have both been shown by the Bone and Signaling Lab to cause bone loss and thus, can be analyzed in parallel to answer our research questions for this senior design project.

4.2 Design Description

Both experiments were conducted in order to determine the effects of dried plum as a countermeasure against the damaging effects of radiation. The timeline of these two experiments can be seen in Figure 1. The only differences between the samples we are analyzing from these two studies are the species of radiation as well as the time point post exposure to radiation at which tissues were collected. For the dried plum + 2Gy gamma experiment, tissues were collected 11 days post IR, while for the dried plum + 1Gy Iron experiment, the specific tissues we will be analyzing were collected at 30 days post IR.

The two studies will be denoted as such in order to differentiate between them: (a) ‘Dried plum + 2Gy gamma’ versus (b) ‘Dried plum + 1Gy Iron.’

4.3 Methods and Materials

*Protocols adapted from Dr. Ann-Sofie Schreurs’ paper “Dried plum diet protects from bone loss caused by ionizing radiation” [11]

4.3.1 Dried Plum + 2Gy Gamma

Animals

The mice utilized for this experiment were male C57BL/6J mice (Jackson Labs, Sacramento, CA). 14 days prior to date of irradiation, mice were randomly assigned by weight to 4 groups (n=8/group). Food and water was available for consumption *ad libitum*. Periodically throughout the experiment, mice were weighed and consumption of food was recorded in order to ensure the maintenance of health of the animals (data not shown). All animal procedures were conducted in accordance with NASA Ames Research Center procedures.

Diets

Control diet was AIN93M, which was the control against the DP-supplemented diet. The custom dried plum diet consisted of the same AIN93M control diet plus the addition of 25% by weight dried plum powder. Both diets were manufactured by Teklad (Madison, WI).

Feeding

14 days prior to irradiation, mice began to be pre-fed on their respective diets and continued until the conclusion of the experiment (Figure 1a). Mice were irradiated at 16 weeks of age and tissues were harvested at 11 days post irradiation.

Radiation Exposure

Mice were exposed to total body irradiation at 16 weeks while conscious with 2Gy Gamma radiation (^{137}Cs at 83cGy/min, JL Shepherd Mark I, NASA ARC). This was performed at NASA Ames Research Center, Moffett Field, CA. Control groups were sham-irradiated, i.e. underwent same procedures as for irradiated group, but were not subject to 2Gy gamma radiation.

4.3.2 Dried Plum + 1Gy Iron

Animals

The mice utilized for this experiment were male C57BL/6J mice (Jackson Laboratories, Bar Harbor, ME). 14 days prior to date of irradiation, mice were randomly assigned by weight to 4 groups (n=10/group). Food and water was available for consumption *ad libitum*. Periodically throughout the experiment, mice were weighed and consumption of food was recorded in order to ensure the maintenance of health of the animals (data not shown). Approval of procedures was granted by the NASA Ames Research Center and the Brookhaven National Laboratory

Institutional Animal Care and Use Committee (IACUC) and conducted in accordance with the health and ethical standards of IACUC.

Diets

Control diet was AIN93M, which was the control against the DP-supplemented diet. The custom dried plum diet consisted of the same AIN93M control diet plus the addition of 25% by weight dried plum powder. Both diets were manufactured by Teklad (Madison, WI).

Feeding

14 days prior to irradiation, mice began to be pre-fed on their respective diets and continued until the conclusion of the experiment (Figure 1b). Mice were irradiated at 16 weeks of age and tissues were harvested at 30 days post irradiation.

Radiation Exposure

Mice were exposed to total body irradiation at 16 weeks while conscious with 1Gy Iron radiation to simulate aspects of space radiation (10cGy/min, at 600 MeV/ion). This was performed at the NASA Space Radiation Laboratory (NSRL) at Brookhaven National Lab (BNL), (Upton, NY). Control groups were sham-irradiated, i.e. underwent same procedures as for irradiated group, but were not subject to 1Gy Iron radiation.

4.4 Results

Body mass

Body mass of all animals was consistently monitored throughout the entirety of the study as indicator of overall health. All animals, for both experiments, showed consistent weight and thus, were considered healthy throughout the duration for the experiment (data not shown).

4.4.1 Dried Plum + 2Gy Gamma

Please refer to Appendix B for table of sample numbers assigned to mice participating in this study as well as their respective treatments conditions: diet and ionizing radiation dose. One animal from this study expired before the end of the experiment and thus, 31 samples will be analyzed. The control diet, sham irradiated, control diet, irradiated, and dried plum, irradiated groups all have a sample size of 8 mice. The dried plum, sham irradiated group has a sample size of 7 mice.

4.4.2 Dried Plum + 1Gy Iron

Please refer to Appendix C for table of sample numbers assigned to mice participating in this study as well as their respective treatment conditions: diet and ionizing radiation dose. In total, 40 samples will be analyzed from this experiment. All experimental groups have a sample size of 10 mice.

4.5 Discussion

The tissues collected from these experiments were the samples we analyzed for our research for the duration of this senior design project.

5. RNA Extraction from Bone

5.1 Introduction

In order to analyze the gene expression of several osteoblast, osteoclast, or oxidative stress related genes, it was first necessary to obtain RNA from the bone, specifically from the left femurs of mice in the ‘Dried plum + 2Gy gamma’ experiment (see chapter 4 for more details). The first phase of this procedure involved the homogenization of bone. Next, it was necessary to wash the homogenate and mix with several chemical reagents (see below). Ultimately, the main priority of this experiment was twofold: to extract high quality RNA (i.e. a high RNA integrity number), and to extract as much RNA as possible. The results of this experiment would greatly impact the following procedures of cDNA conversion and qPCR, and being able to extract more RNA would allow us to convert more cDNA, and thus run more qPCR experiments to test a larger number of genes of interest.

5.2 Key Constraints

The bone homogenization and RNA extraction procedure required several days of work to complete as well as careful handling of the different phases produced. A potential difficulty or inconsistency was the manual homogenization of bone with a handheld homogenizer. Because it cannot be said that every single sample was homogenized for the exact same period of time, to the same degree and because some bones were harder to break down than others, there may have been some inconsistency in terms of the final RNA yield. The RNA extraction procedure was time sensitive and required efficient progression in order to ensure as high RIN as possible. After the three phases were obtained in the test tube (RNA phase, DNA phase, protein phase), it was necessary to treat the samples with extreme care, as separating more than just the RNA phase from the very top would mean drawing other types of molecules or other impurities into our extracted RNA samples.

5.3 Design Description

Homogenization of Bone

After the manual homogenization of mouse femurs, the homogenates were further processed and purified with a Trizol reagent (ThermoFisher Scientific). Trizol reagent contains phenol and

guanidine isothiocyanate to help isolate RNA specifically and moreover inhibits RNase activity. Please refer to the Appendix D for details of protocol. After isolation, RNA was purified with an RNease mini kit (Qiagen, Inc., Valencia, CA, USA). Please refer to the Appendix E for details of RNA cleanup protocol.

Quantifying extracted RNA

Lastly, the concentration of extracted RNA was measured with a Nanodrop spectrophotometer (Nanodrop, Wilmington, DE, USA). Only 1 μ l of sample was required. Subsequent results showed high levels of RNA present (Table 1). These levels were variable from sample to sample, which is why all RNA samples were diluted to 150 ng/ μ l prior to the conversion to cDNA (Appendix F). The absorbance at 260nm (A₂₆₀) measures RNA concentration and absorbance at 280nm (A₂₈₀) measures protein concentration.

Analyzing RNA Quality

RNA Nano Chip - Bioanalyzer (Agilent Technologies) were used to test the quality of all the thirty-one extracted RNA samples (Table 1). A 2100 Bioanalyzer (Agilent Technologies, Santa Clara, CA, USA) was used to read the chip, and produced the respective RNA integrity numbers (RIN) for our samples. For RIN numbers, a value as close to ten as possible is desired, as this signifies RNA of high quality. This procedure was performed on the day after the bone homogenizations and RNA extraction procedures were fully completed.

5.4 Methods and Materials

Please refer to Appendix D, E, and F for complete protocols. RNA was extracted and purified from 31 mouse left femur bones.

5.5 Results and Discussion

The RNA Nano Chip indicated a consistently high integrity for all RNA samples that were extracted from bone (Figure 10, Table 1). This means that the experiment was successful, and the RNA obtained could be used reliably in the next experiment: conversion of RNA to cDNA.

Overall, the concentration of RNA that was extracted was relatively high across all samples, ranging from 47 ng/ μ l to almost 800 ng/ μ l (Table 1). Most samples were between 200

and 300 ng/ μ l. As mentioned before, these samples eventually had to be diluted with distilled water to obtain 150 ng/ μ l, except for the cases where the original concentrations were lower.

These results confirm that the RNA extraction procedure was successful, as we obtained both high quality and for the most part high quantities of RNA. The samples were stored in an - 80°C freezer. The volume that we obtained allowed us to perform cDNA conversion several times for follow up gene expression analyses.

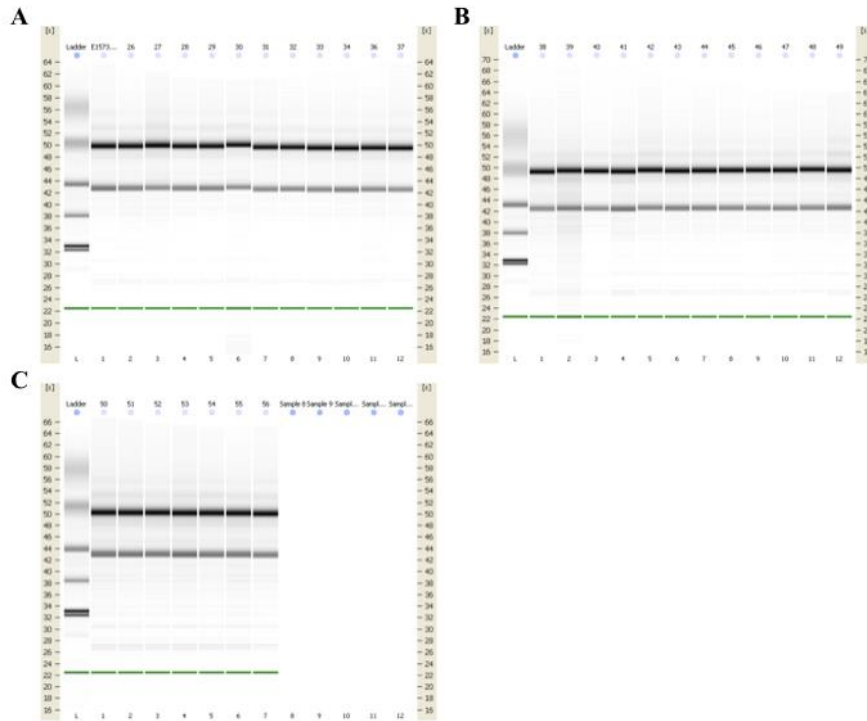


Figure 10. Results from Bioanalyzer gel for 31 RNA samples indicating RNA integrity.

Table 1. Results of RNA concentrations (ng/uL) for each RNA sample ('Dried plum + 2Gy gamma' experiment) via NanoDrop and accompanying RIN#'s via Bioanalyzer.

| Nanodrop and Bioanalyzer Results | | | | | | | |
|----------------------------------|------------------------------------|--------|-------|---------|---------|-------------|------|
| Sample ID | Nucleic Acid Concentration (ng/uL) | A260 | A280 | 260/280 | 260/230 | Sample Type | RIN# |
| d25 | 475.900 | 11.898 | 5.797 | 2.050 | 1.840 | RNA | 10 |
| d26 | 323.600 | 8.090 | 3.909 | 2.070 | 2.100 | RNA | 9.6 |
| d27 | 194.300 | 4.857 | 2.424 | 2.000 | 0.520 | RNA | 9.7 |
| d28 | 411.800 | 10.294 | 5.269 | 1.950 | 1.580 | RNA | 9.9 |
| d29 | 404.000 | 10.101 | 4.976 | 2.030 | 1.600 | RNA | 10 |
| d30 | 79.900 | 1.997 | 1.078 | 1.850 | 0.960 | RNA | 10 |
| d31 | 258.700 | 6.467 | 3.209 | 2.020 | 1.540 | RNA | 9.9 |
| d32 | 251.500 | 6.286 | 3.127 | 2.010 | 1.750 | RNA | 9.9 |
| d33 | 336.300 | 8.406 | 4.070 | 2.070 | 2.040 | RNA | 9.8 |
| d34 | 452.200 | 11.304 | 5.540 | 2.040 | 2.010 | RNA | 9.9 |
| d36 | 169.500 | 4.238 | 2.095 | 2.020 | 1.370 | RNA | 9.5 |
| d37 | 167.900 | 4.198 | 2.076 | 2.020 | 1.820 | RNA | 9.7 |
| d38 | 141.700 | 3.542 | 1.783 | 1.990 | 1.090 | RNA | 9.2 |
| d39 | 47.000 | 1.175 | 0.589 | 1.990 | 1.430 | RNA | 8.8 |
| d40 | 225.100 | 5.628 | 3.042 | 1.850 | 1.180 | RNA | 9.7 |
| d41 | 511.000 | 12.776 | 6.282 | 2.030 | 2.040 | RNA | 9.6 |
| d42 | 187.400 | 4.685 | 2.300 | 2.040 | 1.950 | RNA | 9.5 |
| d43 | 402.600 | 10.066 | 4.891 | 2.060 | 2.070 | RNA | 9.6 |
| d44 | 335.300 | 8.384 | 4.064 | 2.060 | 1.980 | RNA | 9.7 |
| d45 | 467.900 | 11.697 | 5.837 | 2.000 | 1.330 | RNA | 9.6 |
| d46 | 243.000 | 6.075 | 2.978 | 2.040 | 1.720 | RNA | 9.6 |
| d47 | 388.500 | 9.712 | 4.761 | 2.040 | 1.870 | RNA | 9.7 |
| d48 | 227.700 | 5.692 | 2.825 | 2.010 | 1.870 | RNA | 9.5 |
| d49 | 795.600 | 19.889 | 9.376 | 2.120 | 1.590 | RNA | 9.8 |
| d50 | 392.000 | 9.800 | 4.970 | 1.970 | 1.620 | RNA | 9.2 |
| d51 | 323.900 | 8.098 | 4.192 | 1.930 | 1.340 | RNA | 9.6 |
| d52 | 311.200 | 7.780 | 4.023 | 1.930 | 1.340 | RNA | 9.4 |
| d53 | 618.500 | 15.462 | 7.431 | 2.080 | 1.890 | RNA | 9.5 |
| d54 | 280.800 | 7.019 | 3.419 | 2.050 | 1.160 | RNA | 9.6 |
| d55 | 330.100 | 8.253 | 4.127 | 2.000 | 1.760 | RNA | 9.1 |
| d56 | 209.200 | 5.229 | 2.828 | 1.850 | 1.280 | RNA | 9.6 |

6. RNA Conversion to cDNA

6.1 Introduction

Complementary DNA (cDNA) is required for qPCR. The main role of cDNA is to act as a template for the reaction. The cDNA procedure involves the use of a reverse transcriptase, which is the enzyme responsible for generating the complementary strand from a single strand of RNA. The conversion is a straightforward procedure (two-step) that involves the reverse transcription on its own (rather than in combination with the actual PCR), with special optimized buffers and primers. The reaction itself requires several other components, including a buffer to facilitate the reaction, dNTP's, random hexamers, etc. Please refer to the Methods section (Appendix G) for more details. The overarching reason for the RNA to cDNA conversion was because it is required for qPCR, and thus for gene expression analyses in which we hoped to study numerous genes of interest for bone formation or resorption.

6.2 Key Constraints

Our initial cDNA conversion experiments were unsuccessful. The procedure, in general, required meticulous additions and mixes and specific thermocycler program executions throughout its length; perhaps a problem could have been older reagents, primers, or other components or technical mistakes during the procedures. We did not have the time to isolate the specific problem. However, after careful repetition, we finally succeeded. The only other concern during our gene expression analysis was the limited supply of cDNA. Despite limited stocks, we were able to run qPCR for over ten genes in the end.

6.3 Design Description

The cDNA conversion procedure involves addition of different master mixes and other components required for the conventional reverse transcription process. Thirty-one PCR tubes were used for this experiment, one for each sample. It was important to carefully record the progress of reagent addition to each tube so as to ensure the quality and success of the procedure. For more details, please refer to Appendix G.

Success of cDNA conversion can only be elucidated once qPCR has been performed, in which the gene expression graphs are produced, showing successful detection of many different genes of interest. Therefore, success could not be determined in this phase of the project.

6.4 Methods and Materials

Please refer to Appendix G for complete protocol. cDNA was synthesized for 31 mouse left femur bones. RNA utilized for these procedures were the samples extracted and documented in chapter 5.

6.5 Results and Discussion

cDNA was converted at this point in the course of our experiment. There is no concrete validation available because we could not actually determine the success of this procedure until we ran the qPCR and determined whether genes of interest were actually expressed or not. The first time we performed this procedure, we did not succeed; we determined this after the qPCR when it became evident that no genes seemed to be expressed or in general there were no results to speak of (data not shown).

For the cDNA conversions afterwards, we measured the DNA concentration to ensure that there was an adequate level of cDNA present. Though, scientifically, this does not provide actual evidence for successful conversion, and DNA may still be detected in blanks, we still did this and proceeded under the assumption that the cDNA experiments were performed correctly. Therefore, if there was a substantial concentration of DNA detected, then most likely cDNA was converted properly from RNA (data not shown). Our results were further validated by successful detection of genes of interest in qPCR (please refer to results section in chapter 7).

7. Gene Expression Analysis

7.1 Introduction

Quantitative PCR (qPCR) is a measure of actual gene expression and depends on successful RNA extraction and cDNA conversion (chapters 5 and 6). qPCR uses a 5' reporter dye and a 3' MGB quencher, as part of the TaqMan® Probes unique for each gene of interest, to read the expression of a specific housekeeping gene and a gene of interest. When a complementary region of single stranded RNA binds to cDNA, the quencher emits a measurable fluorescent signal. And the process iterates repeatedly for about thirty cycles. Probes for the housekeeping gene and gene of interest have different 5' reporter dyes in order to quantitatively measure differences between their expression levels. Expression levels of our gene of interest (GOI) are compared to a housekeeping gene (HKG). This housekeeping gene is considered a baseline because its expression level remains unaffected when exposed to each of the experimental conditions. For our housekeeping gene, *L19*, the 5' reporter dye was VIC® (Applied Biosystems) and for each of our genes of interest, the 5' reporter dyes was FAM™ (Applied Biosystems).

qPCR can be performed as a one-step reaction in which reverse transcription and PCR is combined in the same tube or in two steps as we did. Two steps, in our case, were favorable for several reasons, which have already been mentioned in chapter 2. Once again, in brief, using separate steps for the reverse transcription and qPCR means that cDNA can be saved and stored for use in the future, as well as optimized buffers can be used for each specific step and therefore increase the quality of the end cDNA or gene expression analysis.

The goal of this procedure was to analyze the measured level of different genes, associated with osteoblast activity (bone formation), osteoclast activity (bone resorption), or oxidative stress (including cell cycle arrest). We hypothesized that genes related to bone formation would be upregulated in the dried plum groups, relative to the controls whereas bone resorption genes should be more prominent in the samples receiving only radiation. The genes that we tested are the following: *Bglap*, *Foxo3*, *Nrf2*, *Postn*, *Sost*, *MTOR*, *Cdkn1a*, *Gadd45a*, *p53*, *BMP2*, *BMP4*, *Rankl*, *Opg*, *Runx2*, and *IGF-1* (refer to Appendix I for more details). Note that these genes were tested from both bone-derived samples as well as bone marrow cells, which had previously been collected before our arrival to the lab. The rationale behind testing bone marrow cells in addition to bone RNA is to observe both how radiation affected the actual

bone marrow cells, precursors that eventually lead to new osteoblast and osteoclast formation, as well as whether dried plum appeared to act on the actual bone marrow (as opposed to only the mineralized bone). Regardless of whether our samples came from bone or bone marrow cells, our expectations remained the same as described above.

7.2 Key Constraints

There are several challenges that we encountered when running qPCR reactions. The very first time that we ran qPCR the results indicated significant noise with little actual gene expression (data not shown). There could have been several reasons for this, but most likely it occurred due to an error in the cDNA conversion procedure (described in chapter 6). Repetition of the cDNA conversion corrected the problems with qPCR.

The samples on which we tested gene expression were collected from mice at 11 days post irradiation. This is a potential drawback to our gene expression analysis because the genes of interest could have or most likely were expressed at a considerable earlier time point after irradiation (i.e. 24 or 48 hours). Because of this, much of our gene expression shows little to no correlation with a few notable exceptions, which will be described in the Results section.

7.3 Design Description

Gene expression analysis was performed in duplicate, and each run tested between three and five genes at a time. The housekeeping gene was added into the same reaction well as the actual gene probes and primers in a 365 well plate. Each qPCR run required specific mixtures of a PCR mastermix, cDNA, primers for genes of interest, and distilled water. For a detailed description of the steps involved, please refer to the Methods section. The qPCR reaction took about one hour and forty-five minutes in most cases and afterwards, the resulting gene expression graphs either validated or negated the expression. The data was processed to convert CT values into gene expression level. Graphs were created and analyzed for statistical significance.

7.4 Methods and Materials

qPCR was performed using the GoTaq® RT-qPCR System (Promega, Madison, WI, USA) and Taqman gene expression assays were utilized (Applied Biosciences, Inc., Foster City, CA, USA). qPCR was performed with a 7300 RT-PCR System (Applied Biosystems, Foster City, CA,

USA). Final volume for each PCR reaction is 10uL. Please refer to Appendix H for protocol. Appendix I details the genes selected and utilized for gene expression analysis. Gene expression levels were calculated relative to the normalized expression levels of ribosomal protein L19 (*RPL19*, assay ID: Mm02601633_g1). Method utilized to calculate these relative expression levels was by the comparative threshold cycle method (DeltaDeltaCt):

$$\text{DeltaCt} = (\text{GOI} - \text{HKG})$$
$$\text{DeltaDeltaCT} = 2^{(-\text{DeltaCt})}$$

qPCR was performed on cDNA of bone samples (derived from bone through steps documented in chapters 5 and 6) as well as on cDNA of bone marrow cells (BMC). The extraction protocol of bone marrow cells from mouse left femur bones, isolation of RNA, and conversion to cDNA is not included in this thesis because this was performed prior to the time we joined the lab (March 2015).

All graphs were formulated using the GraphPad Prism computer program.

Statistics

One-way and two-way analysis of variance (ANOVA) was calculated using JMP computer software analyzing diet and exposure to radiation as the main effects. Results were considered statistically significant if $P < 0.05$ for one-factor ANOVA or for two-factor ANOVA representing an interaction effect.

7.5 Results and Discussion

Gene expression analysis was performed on both bone and bone marrow cell samples. Please note that the RNA was already extracted from the bone marrow cells when we began this project. Therefore, we only had to undertake the extensive RNA extraction procedure previously described for the left femur bone samples.

Figure 11 is a representative image of the raw qPCR data that is reported by the 7300 RT-PCR System (Applied Biosystems, Foster City, CA, USA). This data was then analyzed via the method described in section 7.4. The gene expression data we collected for the genes listed in Appendix I are presented in figures 12-15. Gene expression data was categorized by either being bone remodeling or oxidative damage/cell cycle arrest related genes as well as if performed in Bone or BMC.



Figure 11. Raw qPCR data reported by 7300 RT-PCR System analyzed for gene expression information. Graph shows amplification over time for 4 selected genes of interest and the housekeeping gene (*L19*). Right panel shows all genes we analyzed during this qPCR run.

Of all the genes tested, only three showed a clear, statistically significant correlation. These genes were *Foxo3*, *Rankl*, and *Sost*, all which showed statistically significant results in mineralized midshaft bone.

Foxo3 is a transcriptional activator that is expressed in response to oxidative stress. As can be seen in Figure 15, and was confirmed by one-way ANOVA, IR induces oxidative stress in these bone samples even 11 days post IR. The osteocytes present in these bone samples seemingly have the capacity to retain stress markers even 11 days post IR. This confirms our hypothesis that ionizing radiation, in this experiment 1Gy gamma radiation, induces oxidative stress even 11 days post IR. We are not seeing any effect of dried plum from this analysis of *Foxo3* gene expression in bone.

Rankl, which activates osteoclasts and thus bone resorption activity, increases due to IR. This can be seen in Figure 14 and is confirmed by one-way ANOVA. This indicates that osteoclast activity is heightened when exposed to ionizing radiation and is in response causing osteoclasts to break down more bone in comparison to control. Interestingly though, the addition of the dried plum supplement also showed increased expression of *Rankl*. This is not consistent

with our hypothesis because interpretation would yield that dried plum is increasing resorption, which doesn't explain the bone phenotype of greater bone volume when on the dried plum diet. Our conclusion is that at 11 days post IR a very high rate of bone turnover is occurring, both resorption and formation, and the snapshot we are seeing from our data at day 11 is indicating high levels of bone resorption relative to mice fed control diets and sham-irradiated.

Finally, *Sost*, which encodes a protein that is produced by osteocytes has an anti-anabolic affect on bone formation. This would mean that a high level of *Sost* indicates high levels of bone resorption and suppressed bone formation. Figure 14 indicates that the dried plum diet has an effect on bone formation/resorption. This was confirmed by one-way ANOVA. We are seeing that overall there is an increase in *SOST* expression when on the dried plum diet. As with the results of our *FOXO3* gene expression analysis, since we are analyzing samples at a very late time point, 11 days post IR, the bone is most likely undergoing a high rate of bone turnover and thus the activity of bone formation and resorption is high. Our *SOST* results are just a snapshot of the 11 days post IR gene expression.

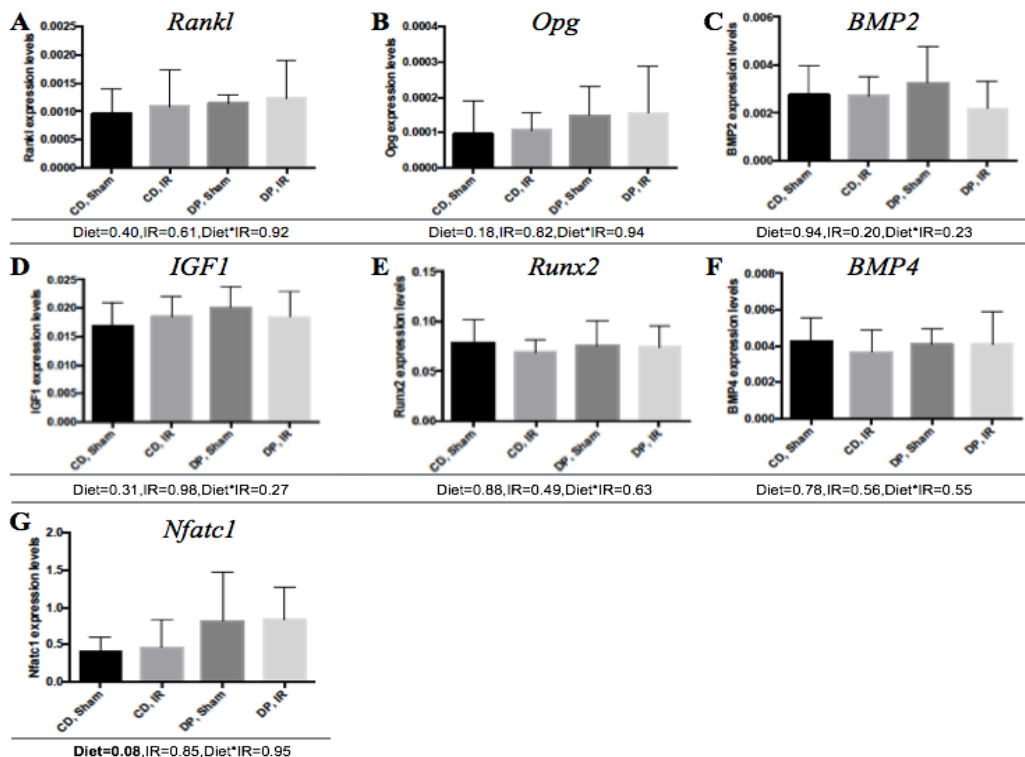


Figure 12. Gene expression of bone related genes in bone marrow cells. Expression levels normalized to L19. IR exposure was 2Gy Gamma radiation. Dried plum (DP) diet was compared to control diets fed (CD) that were either irradiated (IR) or not (sham) (A) *Rankl*, (B) *OPG*, (C) *BMP2*, (D) *IGF-1*, (E) *Runx2*, (F) *BMP4*, (G) *Nfatc1*. Data is represented as mean \pm standard deviation. Bold denotes tendency, but not absolute statistical significance.

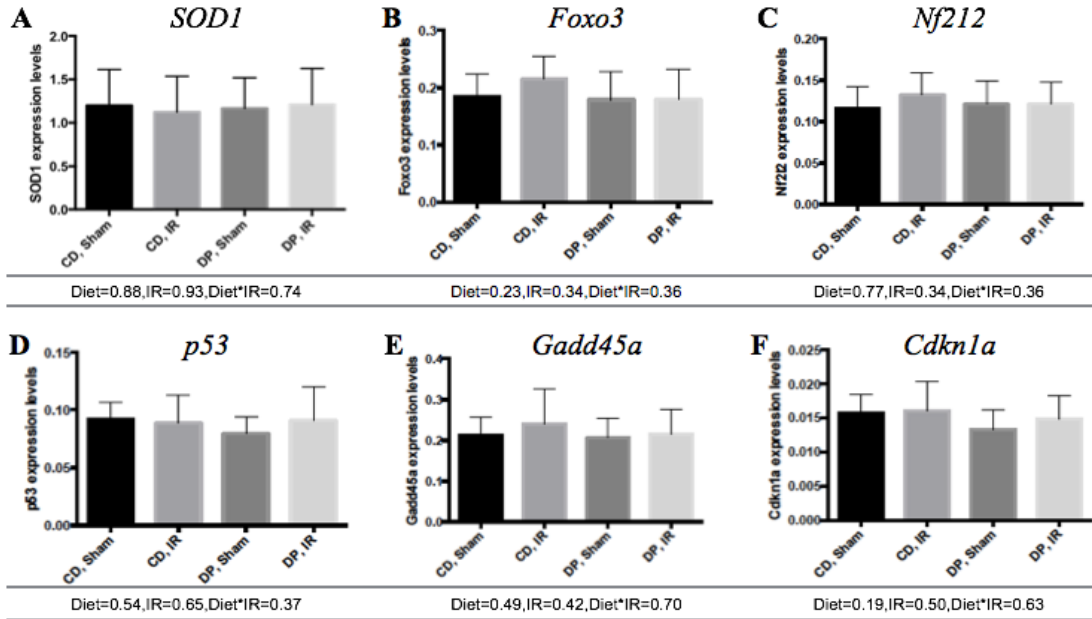


Figure 13. Gene expression of oxidative stress, DNA damage, and cell cycle related genes in bone marrow cells. Expression levels normalized to L19. IR exposure was 2Gy Gamma radiation. Dried plum (DP) diet was compared to control diets fed (CD) that were either irradiated (IR) or not (sham) (A) *SOD1*, (B) *Foxo3*, (C) *Nf212*, (D) *p53*, (E) *Gadd45a*, and (F) *Cdkn1a*. Data is represented as mean \pm standard deviation.

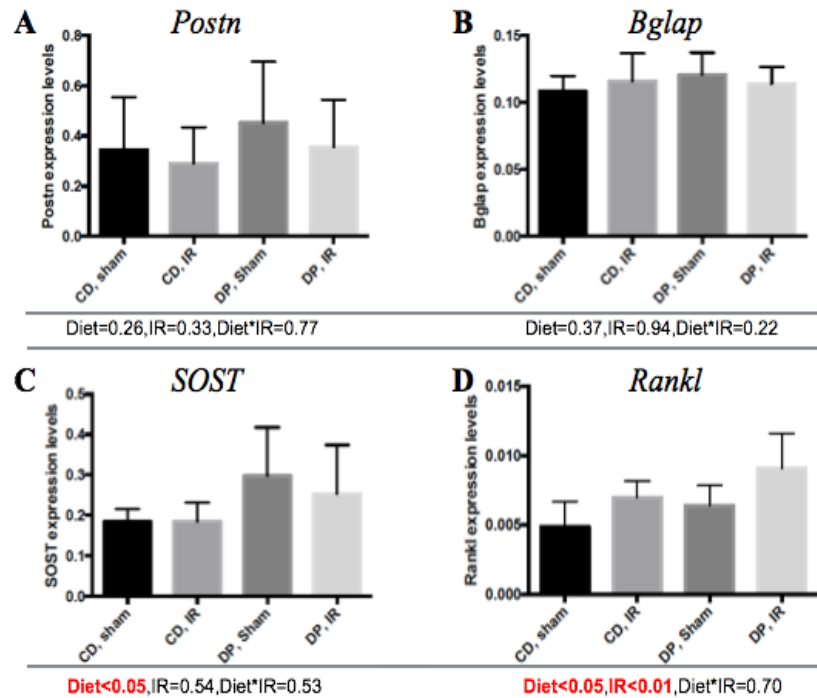


Figure 14. Gene expression of bone related genes in mineralized midshaft bone samples. Expression levels normalized to L19. IR exposure was 2Gy Gamma radiation. Dried plum (DP) diet was compared to control diets fed (CD) that were either irradiated (IR) or not (sham) (A) *Postn*, (B) *Bglap*, (C) *SOST*, and (D) *Rankl*. Data is represented as mean \pm standard deviation. Bold and red denotes statistical significance.

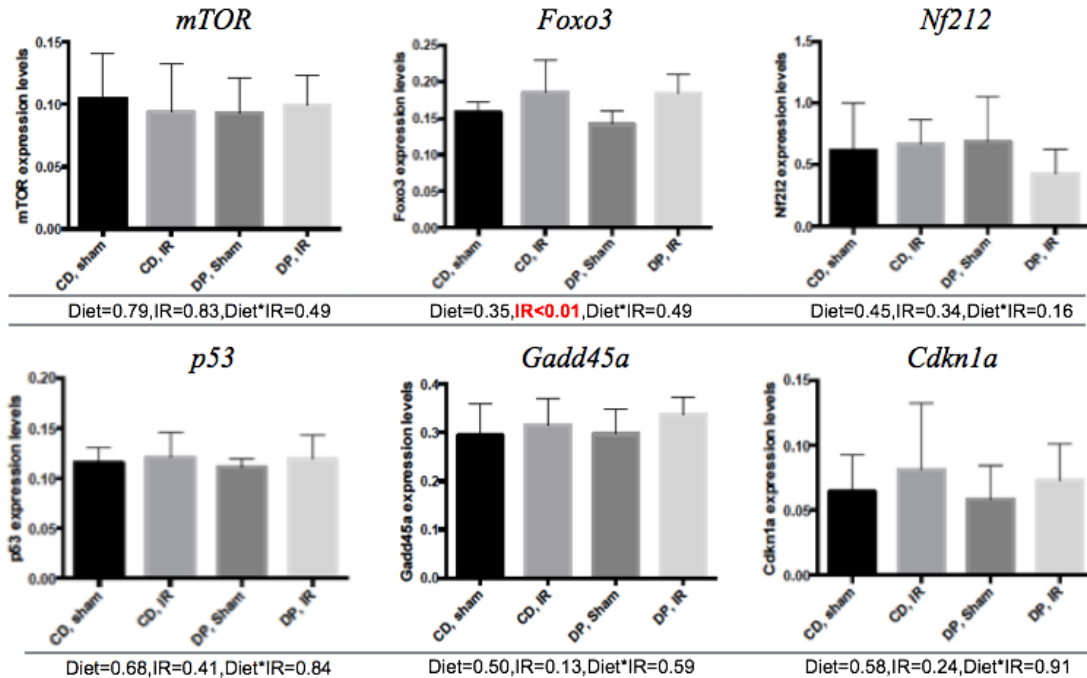


Figure 15. Gene expression of oxidative stress, DNA damage, and cell cycle related genes in mineralized midshaft bone samples. Expression levels normalized to L19. IR exposure was 2Gy Gamma radiation. Dried plum (DP) diet was compared to control diets fed (CD) that were either irradiated (IR) or not (sham) (A) *mTOR*, (B) *Foxo3*, (C) *Nf212*, (D) *p53*, (E) *Gadd45a*, and (F) *Cdkn1a*. Data is represented as mean \pm standard deviation. Bold and red denotes statistical significance.

There were no statistically significant differences in most other gene expression data. There could be several reasons for this. Firstly, it may be that neither radiation nor dried plum significantly affects the specific pathways for the specific genes chose to analyze as of that time. Secondly, it may simply mean that the gene expression was absent at day 11, and so we would need to analyze gene expression of tissues at an earlier time point. It would be informative to repeat the qPCR for all the genes at four different time points, such as 24 hours, 72 hours, 8 days, and 11 days to observe how gene expression changes over time. Another explanation could be that the genes were selected and analyzed were not the right set of genes to fully understand the mechanism of action for how dried plum protects bone. Further analysis and experimentation must be performed to confirm or refute this hypothesis.

Regardless of the true cause(s) for cases where gene expression was not affected by radiation or diet, our gene expression analysis suggests that other directions should be considered to confirm the results shown here. To this end, the next priority in light of these gene expression results was an assay for lipid damage and microCT scanning to analyze the actual physical structure of bones from mice in either the irradiated, dried plum, or control groups.

8. Oxidative Damage Analysis

8.1 Introduction

Ionizing radiation can be particularly harmful because it generates reactive oxygen species that remove electrons from the lipid bilayer of a cell, thereby destabilizing it, and can also damage DNA. The resulting imbalance between free radicals and antioxidant is referred to as oxidative stress. Oxidative stress then leads to oxidative damage. This damage to the lipid bilayer includes lipid peroxidation, in which free radicals remove electrons from the lipids of the cell membrane, thereby leading to its degradation. The attack by free radicals of polyunsaturated fatty acids in the cell membrane sparks a self-propagating chain reaction that destroys more lipids throughout the membrane [21]. The resulting lipid peroxides are unstable and readily decompose to form a variety of compounds, such as malondialdehyde (MDA) [22]. Measuring the MDA levels in a particular sample – whether a tissue homogenate, serum, or other sample type – will provide a reasonable idea of the relative oxidative damage present between samples.

The Thiobarbituric Acid Reactive Substances (TBARS) assay (Cayman Chemical Company) measures MDA levels in a sample of interest. This occurs through the interaction of the thiobarbituric acid reactive substance with MDA. The TBA reagent forms a complex with MDA at a high temperature. This complex can be measured fluorometrically at 530 nm excitation and 550 nm emission wavelengths. Though it can also be measured colorimetrically, there is a higher specificity in the fluorometric analysis [22].

By using the TBARS assay and measuring the MDA levels in samples of serum, bone supernatant, and bone pellet, then normalizing the values to the amount of protein in each sample, we hoped to observe the oxidative damage present in samples from each of four groups: control diet or dried plum diet, irradiated or non-irradiated. The rationale for doing this assay is to determine whether dried plum protects bone by a reduction of MDA levels and to determine the effects of radiation and dried plum beyond the gene expression. We expect to find elevated MDA levels in samples that received radiation without a dried plum diet. If dried plum does, in fact, protect from oxidative damage, then we should expect to find that the dried plum diet groups exhibit an MDA level similar to that of the samples from the control diet, no irradiation group and/or the group that received the dried plum diet without irradiation.

8.2 Key Constraints

There are some constraints that we noted over the course of performing the TBARS oxidative damage experiments.

The TBARS Assay Kit acknowledges that there is some controversy regarding the specificity of the thiobarbituric acid reactive substances [22]. Some believe that TBARS reacts with other compounds, besides MDA, and therefore makes the assay itself somewhat inaccurate. Whether this is the case or not, we decided to run the TBARS assay regardless simply to glimpse at the relative lipid peroxidation between sample groups. Even a general idea of oxidative damage is helpful in our research, as it can potentially support our gene expression and/or microCT results. Specificity to MDA may not be necessary.

We tested all samples in duplicate. After fluorometrically measuring the TBARS reaction plates, we noticed that there were sometimes discrepancies between samples of the same groups. This could be due to variation or lack of uniformity in any of the steps involved: tissue collection methods between different individuals as well as variation in the preparation of the reagents involved such as the color reagent. There may also be variability within the actual mice in the groups as well. The good way to determine the validity of the MDA measurement is to run all samples in triplicate instead.

8.3 Design Description

Before beginning the actual assay, we performed a brief dilution test experiment to determine the optimal dilution factor, if any, to apply to each sample type. For the actual experiments, we tested all forty samples in duplicate. The TBARS experiments were conducted over three separate days. Each of these days focused on a different sample type: serum, bone supernatant, or bone pellet. Bone supernatant refers to the aqueous phase resulting from bone homogenization while the pellet is the solid section of the homogenization. All the necessary reagents were prepared on the day of the experiment. Please refer to the Methods section and Appendix J for more details. An MDA standard was prepared, with concentrations, in μM , of 0, 0.0625, 0.125, 0.25, 0.5, 1, 2.5, and 5. A microBCA assay was also performed on each set of samples on each respective experiment day to obtain information on the total protein concentration and compare it to the proportion of MDA detected.

8.4 Methods and Materials

A BioTek plate reader was used to run the fluorometric MDA measurement scans, at an excitation wavelength of 530nm and an emission wavelength of 550nm as stated by the manufacturer's protocol [22]. Numerous reagents were prepared according to the manufacturer's protocol: TBA acetic acid, sodium hydroxide assay reagent, TCA assay reagent, and the color reagent. The solid thiobarbituric acid reagent and TBA MDA standard were also required. Screw-cap tubes were used for the heating reaction to prevent the caps from otherwise popping open. Samples were heated in heat blocks for one hour before removing. 200µl of sample were added to each well in a 96-well plate, in duplicate for each specific sample. There were forty samples total, belonging to four different experimental groups (control diet or dried plum diet, radiation or non-irradiated). BSA was used as a standard in the microBCA assay that was run concurrently with the TBARS assay. 4 µl of the samples were added to a 96-well plate in duplicate followed by the addition of 80µl of working reagent (prepared according to established lab and manufacturer's protocol).

Statistics

One-way and two-way analysis of variance (ANOVA) was calculated using JMP computer software analyzing diet and exposure to radiation as the main effects. Results were considered statistically significant if $P < 0.05$ for one-factor ANOVA or for two-factor ANOVA representing an interaction effect.

8.5 Results and Discussion

The preliminary dilution experiment for the TBARS assay validated the serum concentration that we used as well as suggested that the dilutions for bone supernatant and bone pellet should be changed. More specifically, the result for MDA in serum indicated that a 1/10 dilution for serums fell well into the desired range (see Figure 16).

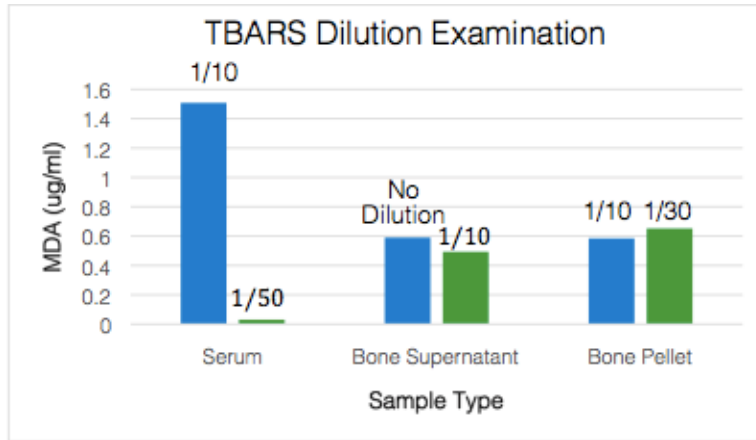


Figure 16. TBARS preliminary experiment for dilution determination. Dilution factor shown above the bars.

Again, from Figure 16, it is also evident that for bone supernatant, a 1/10 dilution is almost the same as the undiluted sample. This may in theory suggest that there was a high level of protein or MDA concentration and that a greater dilution, such as 1/50, is required to determine where the linear range of the TBARS assay is for the bone supernatant samples. However, we ended up decreasing the dilutions because we hoped to see a greater MDA measurement between sample types. A problem with having too diluted samples is that the resulting measured MDA may not be detected well or can be confused with the background.

The first TBARS assay was performed on forty serum samples. The results are shown in Figure 17, below.

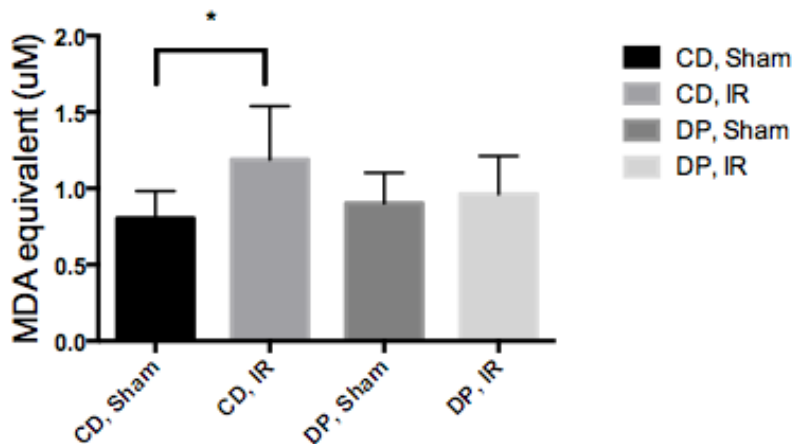


Figure 17. TBARS for Serum samples. IR refers to irradiated groups, which were exposed to 2Gy gamma radiation. CD is the control diet group and DP is the dried plum diet group.

The MDA level normalized to protein for the group that received the control diet and 2Gy of gamma radiation is significantly higher than the control diet group that was not

irradiated. Both of the dried plum diet groups also have lower MDA levels, closer to the control level. Therefore, dried plum prevented a radiation-induced rise in serum MDA levels. These findings suggest that a potential mechanism by which dried plum protects bone is through a systemic reduction of oxidative damage, a trend that is present in the blood circulation. This is promising because an effect on the serum also suggests that dried plum may possess beneficial effects for other tissues or organs beyond just the bones.

In the case of the TBARS assays for bone supernatant and pellet samples, there was no increase in MDA levels after irradiation as had been expected and seen before. Dried plum did not appear to impart any bone-protective effects either. We cannot draw any conclusions from the data for bone supernatant and bone pellet samples. This may, again, be related to inconsistent tissue collection at the time when the different tissues were collected or to other possible variability's in the individual reagent preparation during each of the three times this experiment was set up and performed. A way to confirm these results is to re-run the TBARS assay to determine whether the statistical insignificance and/or unexpected trends remain and to look at other assays that can detect more stable or different types of oxidative damage, beyond lipid peroxidation.

9. Micro-Computed Tomography

9.1 Introduction

Ionizing radiation damages the integrity of the micro-architecture of bone. Micro-computed tomography (microCT) is the gold standard for assessing bone morphology and micro-architecture. This method utilizes high-resolution x-ray measurements taken at all angles around your sample, to build a full, 3D reconstruction of your sample [23]. The sample is then characterized by how material density within the image is distributed. This procedure is much more accurate than 2D analysis, is not destructive to the sample itself, and can be performed as high-throughput unlike many other morphology study methods. Thus, microCT was chosen as the method to physically characterize our bone samples. After recreating 3D images of mice lumbar 4 (L4) vertebrae, investigation of how dried plum protects the bones micro-architecture from the damaging effects of radiation can take place. MicroCT allowed us to quantify the 3D micro-architecture of the cancellous tissue of the L4 vertebral body (Figure 18). Rod and plate-like structures called trabeculae make up the cancellous tissue. Quantification and characterization of these trabeculae is the main interest for data analysis from microCT.

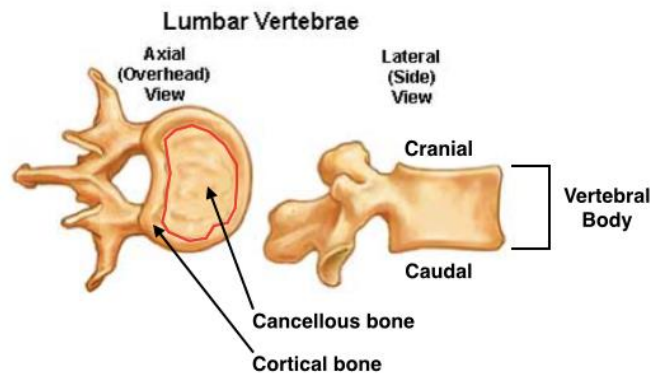


Figure 18. Lumbar Vertebrae highlighting important locations and directions. [25]

The laboratory with which we partnered for this senior design project has already determined that dried plum successfully protects the appendicular skeleton, the long bones (ex. tibia). Under investigation, and an important element of our research goal, is to determine the ability of dried plum to protect the axial skeleton (ex. vertebrae) as well. Before making any conclusions or comparisons between the effects of dried plum on the axial versus appendicular skeleton, we had

to characterize all our samples and first, make comparisons between the control and experimental groups of just the vertebrae samples.

9.2 Key Restraints

The MicroCT SkyScan 1174 utilized for scanning our vertebra samples utilizes x-ray to perform the scanning. Because we were working in a room that x-ray's were being emitted, there was a long training period that took place before any scanning or analysis of our samples via computer programs could take place. After training for many consecutive days, we were finally able to begin the scanning and post-processing, which in order to accomplish in time for our senior design presentation, was very rushed.

Visual self-check

After scanning but prior to any post-processing, we had to go through and check a few slices to ensure that there were no smudges or abnormal bright spots on the scans. The presence of these obstructions is a result of the microCT misaligning the bone slice images during the scanning process. These smudges or bright spots could be misinterpreted as false trabecula during analysis. Thus, if a significant number of smudges were identifiable while spot-checking a few locations within the vertebral body from an individual bone, rescanning of that bone would need to occur. We unfortunately needed to rescan approximately 6 vertebrae to ensure that false trabecula would not interfere with our results.

Determining a Standard 'Region of Interest' For All Samples

Post-processing includes reconstruction of all x-ray images that are taken during scanning (1000 image slices), rotating the reconstructed vertebrae to be aligned with cranial direction at the top and caudal at the bottom with major access of rotation at the center of the vertebral body (Figure 18). After reconstruction and re-alignment, contouring of the cancellous bone can begin. Only a specific region of interest of this cancellous bone will be contoured. A key constraint to determining the location of this region of interest is the location of a specific vertebra's growth plate at the cranial and caudal locations. None of the growth plate should be included as part of the region of interest. Lab protocols used for previous experiments in our lab utilized the standard that, at the bone slice where the caudal growth plate transitions to visible trabeculae,

add a 50 slice buffer to the above number, which will then be the bottom of the region of interest and then add 300 slices above the 50, with this being the top of the region of interest. Trial and error indicated that these constraints would not work for the vertebrae that we were trying to contour. The vertebral body was too small, that 300 slices above the 50 slice buffer region landed us in the cranial growth plate. In order to ensure that no growth plate would be visible in our region of interest we had to try many different parameters. Initially we tried decreasing the buffer region, which would lend itself successful to one bone and then when we moved on to contouring the next, where it became apparent that the parameters were now not applicable. Finally, before jumping into the contouring, we went through all 40 vertebrae and determined what parameters for the region of interest would be applicable to all of the samples. Finally we were able to settle on a procedure where the bottom of our region of 260 slices above this point constituted the top of our region of interest.

Division of Labor

Due to the large number of samples that we needed to scan, reconstruct, contour, and analyze (40 samples total) we had initially decided to split the samples into 2 sets: samples d1-d20 and d21-d40 constituted the two groups. Each set included 5 samples from each of the 4 experimental groups, which we were comparing. We wanted to do this so that both of us team members would have the opportunity to take part and perform all steps necessary to go from scanned vertebrae to data collection and 3D image generation. Although, normally, it is best for one individual to perform all analysis, due to the fact that we all have slightly different methods even while following the exact same protocols, we decided to split the tasks evenly to both be equally involved in the process as well as to divide up the significant amount of labor. After the contouring stage, at which point data can be calculated for various parameters detailed later in this section, it became apparent that our methods were not 100% identical and because of this we were getting slight variation in results. In order to ensure consistency and reliability of the data, we decided to start again and this time we would analyze the other person's samples and then compare results sample to sample. After completion, we now had two sets of results for each sample. In reality, there were some slight differences between the 2 sets, but the outputs were the same. In order to decide which set of data was to be selected as the final results, the standard

deviations of the results for each experimental group were compared and the results with the tightest spread (i.e. lowest standard deviation) would be utilized.

9.3 Design Description

The ultimate goal of this phase of our project was to determine if dried plum protects against ionizing radiation any differently in the axial skeleton (ex. vertebrae) in comparison to the appendicular skeleton (ex. tibia or femur). Please refer to sections 4.3.2 and 4.4.2 for information regarding the animals and experimental design of the study from which samples were analyzed by microCT.

Before any quantification can be performed comparing amount of bone loss caused by radiation exposure either on the control diet or the dried plum diet, there are many post-processing steps that must be completed. The timeline of procedures for bone micro-architecture analysis by microCT can be broken down into 6 steps:

Step 1: Scanning (Skyscan 1174)

Step 2: Bone Reconstruction (NRecon)

Step 3: Rotating/Re-alignment (DataViewer)

Step 4: Contouring (CTAn)

Step 5: Quantification (BATMAN)

Step 6: Final 3D Image Generation (CTVol)

The information in the parentheses denotes the instrument or computer program utilized to perform each step.

9.4 Methods and Materials

9.4.1 Step 1: Scanning

Vertebrae samples previously fixed and then stored in 70% Ethanol, then were transferred to phosphate-buffered saline (PBS) solution 24 hour prior to scanning. Scanning was performed utilizing a SkyScan 1174 microCT scanner (Kontich, Belgium) with a 10.5 μm resolution. 1000 image slices are taken for each of the vertebra samples. Overall, 40 vertebrae were scanned for this experiment.

9.4.2 Step 2: Bone Reconstruction

Reconstruction is performed to compile all image slices taken by the scanning machine into one volume. This reconstruction is selected for a region beginning 100 slices above and below the vertebrae (data not shown). Spot checks of a few slices within the vertebrae image were performed to ensure that image was clean and without smudging or bright white spots that could potentially interfere with later results. These spot checks were performed with a bottom limit of 0 and an upper limit of 0.16. If spot checks pass, the selected volume can be sent for reconstruction by the NRecon computer program. If spot checks do not pass, vertebrae must be rescanned.

9.4.3 Step 3: Rotating/Re-alignment

After reconstruction is complete, re-alignment of the whole volume can be performed to ensure that all samples are being analyzed with the same orientation. This is performed utilizing the DataViewer computer program. All vertebrae are re-aligned so that the cranial growth plate is on top, the caudal growth plate is at the bottom, and the axis of rotation is at the centerline of the vertebral body.

9.4.4 Step 4: Contouring

Within the reconstructed volume of the whole vertebra sample, only a specific region of interest within the vertebral body will be analyzed.

Region of Interest

To determine the region of interest that was analyzed for all 40 samples, in the CTAn computer program, first start at the caudal growth plate. Move cranial through the growth plate until you do not see any more of the growth plate at all. This slice number is set as “the bottom of selection.” Now calculate 260 slices above this bottom selection point (data not shown). This new slice number is set as “the top of selection.” This is now the region of interest that will be contoured for data analysis. For the cancellous bone, a region of interest, 1.7mm distal to the caudal growth plate of the L4 vertebrae, was selected and included in our analysis (Figure 19).

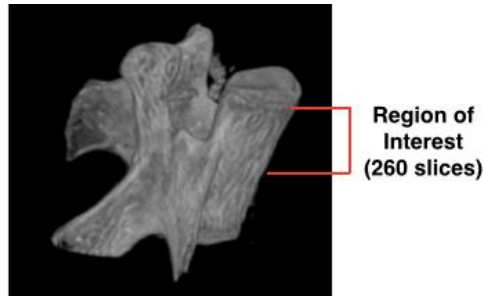


Figure 19. Lumbar 4 vertebrae with region of interest highlighted within the vertebral body.

Contouring

Utilizing the screen extension pad and pen as well as utilizing the CTAn computer program, draw a region of interest around the cancellous bone of the vertebral body at the top and bottom selections that were made above – keeping note to keep a constant space between the region of interest and the cortical wall. This region of interest will be automatically interpolated from top to bottom by the computer program. If this interpolated region of interest starts to deviate from encompassing just the cancellous bone, beginning to touch the cortical bone, a new, adjusted region of interest must be drawn. These adjustments must be made throughout the entire vertebrae, from top of selection to bottom of selection. When complete, the entire contoured regions are saved as a volume of interest.

9.4.5 Step 5: Quantification

Image processing and quantification of our 3D parameters of interest is performed via BATchMANager (BATMAN) computer program. This program allows you to select your region of interest for all samples and then as one, perform analysis on the whole batch. This analysis is directed by a “task list” created by the user, which directs the computer on how the samples are to be analyzed with what conditions, what calculations are to be performed for relevant parameters and where to save the data when the program is complete.

In order to quantify the extent of bone loss when on the dried plum supplemented diet, in comparison to control samples, multiple parameters were analyzed including, but not limited to, bone volume to total volume (BV/TV), trabecular thickness (Tb.Th), trabecular separation (Tb.Sp), and trabecular number (Tb.N). These parameters as well as a few others are described below (*3D Micro-architecture parameters of interest* section).

3D Micro-architecture parameters of interest

Please refer to Appendix K for a table of all parameters of interest that were analyzed from the contoured regions of interest for all vertebrae samples.

Statistics

One-way and two-way analysis of variance (ANOVA) was calculated using JMP computer software analyzing diet and exposure to radiation as the main effects. Results were considered statistically significant if $P < 0.05$ for one-factor ANOVA or for two-factor ANOVA representing an interaction effect.

9.4.6 Step 6: Final 3D Image Generation

After contouring our region of interest within the vertebral body of the L4 vertebrae, all the contoured slices could be reconstructed into a volume of interest. This volume of interest was transferred into a program called CTvol. CTvox combined all the images to recreate and render a 3D representation of the vertebra, based on our slice-by-slice regions of interest. We were able to use this 3D rendition to compare the physical characteristics and orientation of the trabeculae within the L4 vertebrae of different groups. From the 3D structure we could visualize differences in trabecular thickness or density of the bone within in the vertebral body between experimental groups.

9.5 Results & Discussion

9.5.1 Quantification

From the task list executed by BATMAN we were able to quantify of our 3D micro-architecture parameters of interest for all 40 samples. All results acquired from the microCT were analyzed using a 1-factor ANOVA and revealed the following results (Figure 20). Raw data from this quantification of 3D micro-architecture parameters is not shown. Analysis of bone volume over total volume (BV/TV) showed a 9% increase for mice on the dried plum diet. Analysis of trabecular thickness (Tb.Th) also showed a 9% increase for mice on the dried plum diet. Data did not reveal a statistically significant change in trabecular separation (Tb.Sp), trabecular number (Tb.N), connectivity density (Conn.D), or structure model index (SMI). Regardless, data is presented in figure 20.

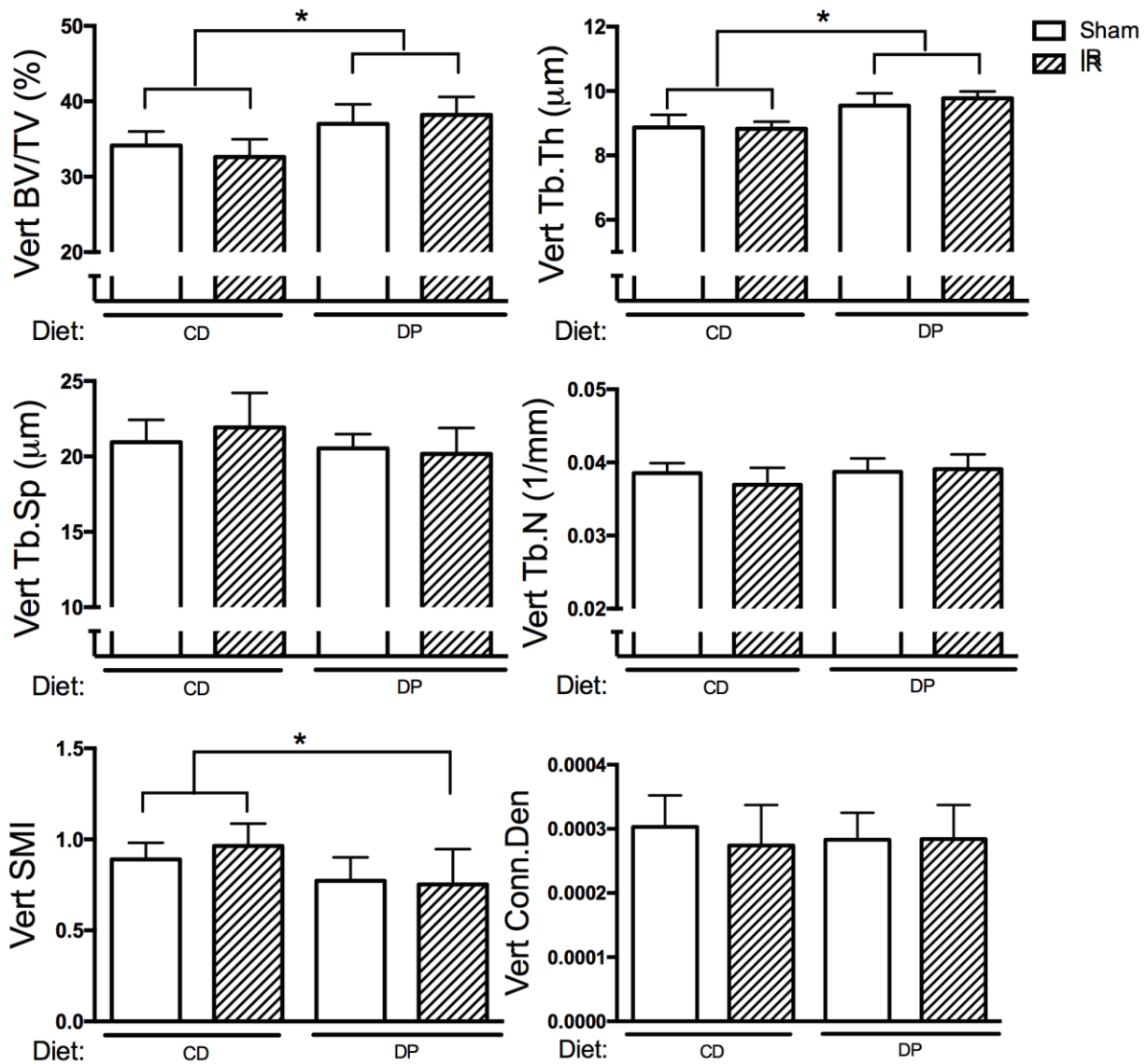


Figure 20. Quantitative morphometry data determined by microCT for vertebrae (appendicular skeleton). CD stands for control diet, DP stands for dried plum, and IR for this experiment was 1Gy Iron radiation. BV/TB = bone volume over total volume, Tb.Th = trabecular thickness, Tb.Sp = trabecular separation, Tb.N = trabecular number, Conn.D = connectivity density, and SMI = structure model index. Data shown are mean \pm standard deviation (n=10) and analyzed by 1-factor ANOVA. *Indicates $p < 0.05$ statistical significance.

Contouring and analysis was also performed for tibia samples from the same experimental design. Quantified data for our parameters of interest can be seen in Figure 21. Analysis of BV/TV data of the tibia shows a statistically significant radiation induced bone loss. Radiation is seen to have an effect on the appendicular skeleton (i.e. tibia). This bone loss was not seen for the axial skeleton (i.e. vertebrae). BV/TV stays consistent for both dried plum

groups, sham and 1Gy Iron irradiated (Figure 21). This data shows radiation induced bone loss is mitigated by a dried plum supplemented diet.

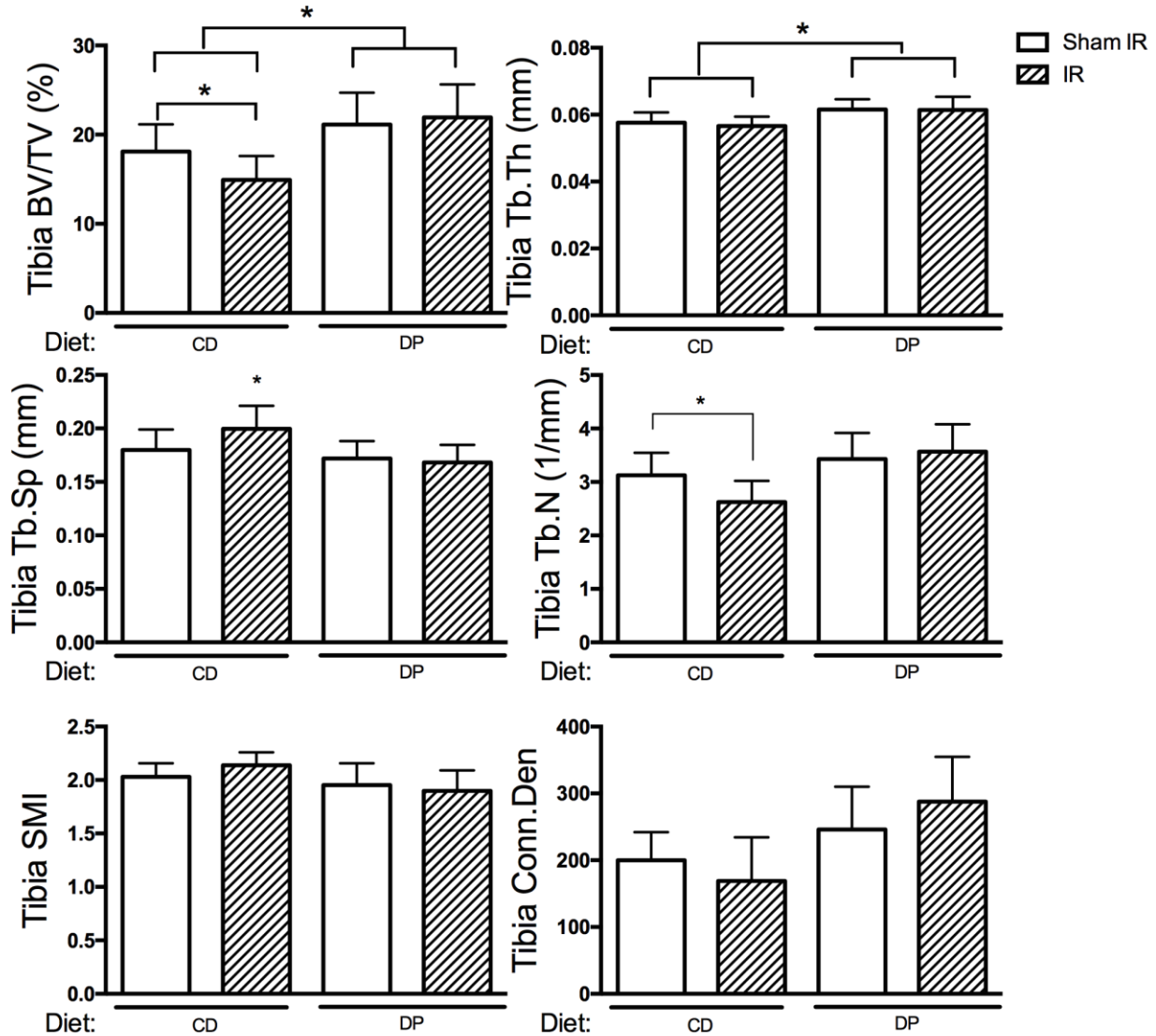


Figure 21. Quantitative morphometry data determined by microCT for tibia (axial skeleton). CD stands for control diet, DP stands for dried plum, and IR for this experiment was 1Gy Iron radiation. BV/TB = bone volume over total volume, Tb.Th = trabecular thickness, Tb.Sp = trabecular separation, Tb.N = trabecular number, Conn.D = connectivity density, and SMI = structure model index. Data shown are mean \pm standard deviation (n=10) and analyzed by 1-factor ANOVA. *Indicates p<0.05 statistical significance.

9.5.2 3D Images

From the 3D reconstructions of the scanned trabeculae by CTvox, we were able to visualize differences in bone micro-architecture from each experimental condition. A set of representative

images can be seen in Figure 22, which illustrates one 3D reconstructed image per experimental condition.

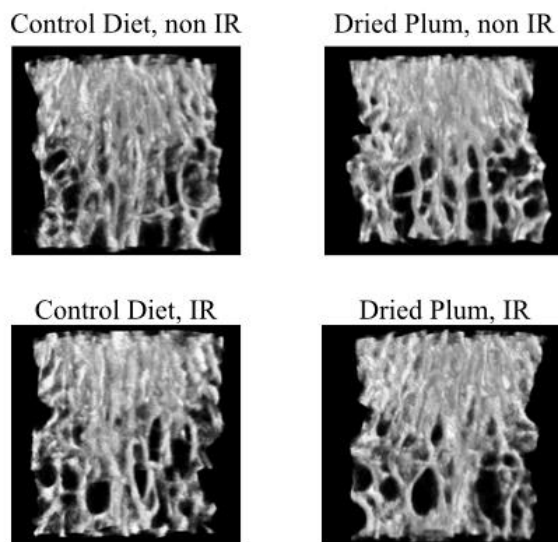


Figure 22. Representative images of 3D reconstruction of cancellous bone micro-architecture via microCT.

Both groups of mice on the dried plum diet had statistically significant higher bone volume and trabecular thickness in comparison to CD-fed controls. Results did not indicate any significant decrease in vertebrae BV/TV or Tb.Th for mice on the control diet that were irradiated with Iron (Figure 20). Specifically in the vertebrae, IR is not causing any tissue loss. In contrast, data acquired from analysis of the tibia, which is part of the appendicular skeleton, specifically BV/TV, showed that ionizing radiation caused a significant amount of bone loss due to IR when on the control diet in comparison to the dried plum supplemented diet (Figure 21). Conclusion can be stated that in the appendicular skeleton, dried plum imparts a radio-protective effect on bone, while dried plum only functions to increase bone mass in the axial skeleton, independent of radiation exposure. Another explanation could be that the tibia and the vertebrae have different rates of remodeling and different reaction times to IR. Analysis of the 3D reconstructed images of the bones micro-architecture we could definitively see that in comparing samples from the control diet and dried plum supplemented diet that were non-irradiated, the upper section of the bone is more densely packed in the dried plum group (Figure 22). Between the same images, trabecular thickness is significantly greater for the dried plum group compared to control. In combination, the data as well as the 3D images that we collected in analysis of the axial skeleton, specifically the vertebrae, showed improvement in bone structure and increase in

bone mass for the dried plum group, but this improvement is not directly because of dried plums ability to protect from ionizing radiation. A diet supplemented with dried plum promotes acquisition of bone mass independent of radiation for the mice in this experiment.

Because we did not see a significant decrease in bone volume and trabecular thickness for the irradiated control diet group in comparison to the non-irradiated, we cannot make any conclusions on the protective effects of dried plum on the micro-structure of the bone of the axial skeleton after exposure to irradiation. A possible reason for not seeing this radiation induced bone loss may be because the 1Gy Iron radiation dosage was not strong enough to cause significant changes in physical bone morphology. In contrast, we can state that our results support that dried plum is able to protect the appendicular skeleton from radiation induced bone loss.

10. Conclusions

10.1 Summary

There are several things that we can conclude from the experiments that we performed for this research project over the past year.

Firstly, we found that radiation increases both bone resorption and oxidative stress. Our gene expression results pointed to an increase in genes associated with resorption (i.e. *Rankl*). Gene expression of *Foxo3*, a marker for oxidative stress, increased as well. Many of the genes that we tested yielded statistically insignificant results, probably because the tissues that we tested were collected at a late time point after irradiation. Please refer to chapter 7.

The TBARS assay was performed to gauge the level of oxidative damage in serum, bone supernatant, and bone pellet samples. For the serum samples, MDA levels were elevated in the control diet, 2 Gy gamma radiation group, relative to the control and all other groups in general. This suggests that a potential mode of action by which dried plum protects bone is a systemic reduction of oxidative damage. The TBARS results for both supernatant and pellet were inconclusive.

Our results with the microCT were particularly interesting because not much attention has been devoted to the interaction between dried plum, radiation, and the axial skeleton, in our case the L4 vertebra. The results that we obtained cannot confirm a bone-protective effect from dried plum because there was no radiation-induced bone mass decrease to begin with. Though the conditions that we used in our experiment cannot confirm this, performing this experiment with a higher level of radiation may provide greater insights as to whether dried plum can actually protect vertebrae. What we did find, however, is that dried plum successfully increases the bone mass of the axial skeleton, independent of radiation or any other factors. This is significant partly because it demonstrates that dried plum on its own, under normal conditions, can contribute to a greater bone mass and overall a promotion of bone health.

10.2 Future Work

The experiments we were able to conduct over the past year are not sufficient to fulfill our goal of fully understanding how dried plum protects bone from radiation. There are numerous other experiments that we can perform to better understand the nature of dried plum.

Immunohistochemistry staining, such as hydroxyguanosine (8-OHG) staining, can be performed on slices of bone tissues from representative condition groups to analyze oxidative damage to DNA within bone cells. In an antibody-antigen interaction, antibodies can bind specific regions of DNA within the nucleus or to other specific antigens. The stain can then be analyzed for differences between irradiated tissue and control tissue and the overall cell morphology.

A follow-up to the micro-CT staining could be mechanical testing to quantify the mechanical properties of vertebrae, in relation to a dried plum diet relative to the control or irradiation relative to the sham control groups. By applying a certain load onto these vertebrae, we can determine the strength of these bones before they fracture.

Running assays to test DNA-damage may also be helpful, as it would confirm whether radiation-induced oxidative stress and damage affects the DNA directly. A possible assay for this could be the 8-oxoguanine assay, which would test for a characteristic DNA lesion that is typically induced by reactive oxygen species. In this way, we could examine the extent to which reactive oxygen species damages DNA and therefore the gene expression of genes related to bone formation, resorption, and oxidative stress.

The last phase of our research project that we would have liked to conduct includes the extraction and purification of the active components from dried plum, followed by *in vitro* experiments to test the effects of these components on cell cultures to fully identify the component responsible for bone protection. After extracting dried plum polyphenols or other potential active components, they can be applied to the media of cell culture cells of bone marrow derived cells either alone or in conjunction with irradiation to observe which components seem to impart a beneficial effect for the cells. A possible method to extract dried plum polyphenols has already been cited by Bu et al. [15].

10.3 Concluding Remarks

Over the course of this past year, we were able to conduct three main phases of our research: gene expression with qPCR, oxidative damage analysis with the TBARS assay, and physical characterization with microCT scans. This is not sufficient to get the full picture of how dried plum protects bone. However, suggested experiments to continue this research appear in the previous section.

At this point, dried plum remains a very promising dietary option to protect bone from radiation. Though further research is required to understand its function better, even preliminary results suggest that dried plum is very capable of protecting the bones of astronauts, and other patients suffering from bone conditions such as osteoporosis. Dried plum even appears to promote bone mass in some cases, as described in chapter 9.

We look forward to seeing how this project progresses beyond our senior design thesis, in the years to come. We hope to see how researchers in our lab at NASA Ames as well as other labs continue to advance the general understanding of the mechanisms of dried plum and discover other potential solutions that will one day promote the health of astronauts and facilitate longer-term missions to Mars and beyond.

We are very grateful for having received this amazing opportunity to undertake this yearlong research project in the Bone and Signaling Laboratory of NASA Ames Research Center.

11. Appendices

Appendix A. Budget

Table 2. Complete itemized estimated costs for all reagents utilized for our experiments. *These costs as well as this research was supported by National Space Biomedical Research Institute grant #MA02501 (RKG, CL, JSA) under NASA cooperative agreement NCC 9-58, a DOE-NASA Interagency Award #DE-SC0001507, supported by the Office of Science (BER), U.S. Department of Energy (RKG), and a NASA Postdoctoral Program fellowship

| Item\ | Cost |
|---|---------------|
| RNAase free water | \$10 |
| Trizol | \$50 |
| Chloroform | \$50 |
| Ethanol | \$25 |
| RNEasy Mini Kit (Qiagen) | \$1000 |
| Random Hexamers | \$100 |
| dNTP's | \$75 |
| 5x Standard Buffer (cDNA) | \$20 |
| DTT | \$20 |
| RNAse Out | \$50 |
| Reverse Transcriptase | \$100 |
| TaqMan Gene Expression Primers (x18 primers) | \$1500 |
| TBARS kit | \$350 |
| PBS | \$25 |

Appendix B. Respective Experimental Conditions for ‘Dried Plum + 2Gy Gamma’ Experiment mice.

Table 3. Assigned diet and radiation condition for all mice from ‘Dried plum + 2Gy gamma’ experiment. d25-d56 indicate the dissection ID given to each of the mice. Please note that mouse d35 passed away during the experiment and thus no samples were collected.

| Dissection ID | Diet Full Name | IR | Combined Treatment |
|---------------|-----------------------------|------------|--------------------|
| d25 | Ctrl-P - AIN93M | Sham | CD, Sham |
| d26 | Ctrl-P - AIN93M | 2 Gy gamma | CD, 2Gy |
| d27 | Plum - Plum powder diet 25% | Sham | DP, Sham |
| d28 | Plum - Plum powder diet 25% | 2 Gy gamma | DP, 2Gy |
| d29 | Ctrl-P - AIN93M | Sham | CD, Sham |
| d30 | Ctrl-P - AIN93M | 2 Gy gamma | CD, 2Gy |
| d31 | Plum - Plum powder diet 25% | Sham | DP, Sham |
| d32 | Plum - Plum powder diet 25% | 2 Gy gamma | DP, 2Gy |
| d33 | Ctrl-P - AIN93M | Sham | CD, Sham |
| d34 | Ctrl-P - AIN93M | 2 Gy gamma | CD, 2Gy |
| d36 | Plum - Plum powder diet 25% | 2 Gy gamma | DP, 2Gy |
| d37 | Ctrl-P - AIN93M | Sham | CD, Sham |
| d38 | Ctrl-P - AIN93M | 2 Gy gamma | CD, 2Gy |
| d39 | Plum - Plum powder diet 25% | Sham | DP, Sham |
| d40 | Plum - Plum powder diet 25% | 2 Gy gamma | DP, 2Gy |
| d41 | Ctrl-P - AIN93M | Sham | CD, Sham |
| d42 | Ctrl-P - AIN93M | 2 Gy gamma | CD, 2Gy |
| d43 | Plum - Plum powder diet 25% | Sham | DP, Sham |
| d44 | Plum - Plum powder diet 25% | 2 Gy gamma | DP, 2Gy |
| d45 | Ctrl-P - AIN93M | Sham | CD, Sham |
| d46 | Ctrl-P - AIN93M | 2 Gy gamma | CD, 2Gy |
| d47 | Plum - Plum powder diet 25% | Sham | DP, Sham |
| d48 | Plum - Plum powder diet 25% | 2 Gy gamma | DP, 2Gy |
| d49 | Ctrl-P - AIN93M | Sham | CD, Sham |
| d50 | Ctrl-P - AIN93M | 2 Gy gamma | CD, 2Gy |
| d51 | Plum - Plum powder diet 25% | Sham | DP, Sham |
| d52 | Plum - Plum powder diet 25% | 2 Gy gamma | DP, 2Gy |
| d53 | Ctrl-P - AIN93M | Sham | CD, Sham |
| d54 | Ctrl-P - AIN93M | 2 Gy gamma | CD, 2Gy |
| d55 | Plum - Plum powder diet 25% | Sham | DP, Sham |
| d56 | Plum - Plum powder diet 25% | 2 Gy gamma | DP, 2Gy |

Appendix C. Respective Experimental Conditions for ‘Dried Plum + 1Gy Iron’ Experiment mice.

Table 4. Assigned diet and radiation condition for all mice from ‘Dried plum + 1Gy Iron’ experiment. d1-d40 indicate the dissection ID given to each of the mice.

| Dissection ID | Diet | IR | Combined Treatment |
|---------------|------------|-----------|--------------------|
| d1 | Control | Sham | CD, Sham |
| d2 | Control | 1 Gy iron | CD, 1 Gy |
| d3 | Dried Plum | Sham | DP, Sham |
| d4 | Dried Plum | 1 Gy iron | DP, 1 Gy |
| d5 | Control | Sham | CD, Sham |
| d6 | Control | 1 Gy iron | CD, 1 Gy |
| d7 | Dried Plum | Sham | DP, Sham |
| d8 | Dried Plum | 1 Gy iron | DP, 1 Gy |
| d9 | Control | Sham | CD, Sham |
| d10 | Control | 1 Gy iron | CD, 1 Gy |
| d11 | Dried Plum | Sham | DP, Sham |
| d12 | Dried Plum | 1 Gy iron | DP, 1 Gy |
| d13 | Control | Sham | CD, Sham |
| d14 | Control | 1 Gy iron | CD, 1 Gy |
| d15 | Dried Plum | Sham | DP, Sham |
| d16 | Dried Plum | 1 Gy iron | DP, 1 Gy |
| d17 | Control | Sham | CD, Sham |
| d18 | Control | 1 Gy iron | CD, 1 Gy |
| d19 | Dried Plum | Sham | DP, Sham |
| d20 | Dried Plum | 1 Gy iron | DP, 1 Gy |
| d21 | Control | Sham | CD, Sham |
| d22 | Control | 1 Gy iron | CD, 1 Gy |
| d23 | Dried Plum | Sham | DP, Sham |
| d24 | Dried Plum | 1 Gy iron | DP, 1 Gy |
| d25 | Control | Sham | CD, Sham |
| d26 | Control | 1 Gy iron | CD, 1 Gy |
| d27 | Dried Plum | Sham | DP, Sham |
| d28 | Dried Plum | 1 Gy iron | DP, 1 Gy |
| d29 | Control | Sham | CD, Sham |
| d30 | Control | 1 Gy iron | CD, 1 Gy |
| d31 | Dried Plum | Sham | DP, Sham |
| d32 | Dried Plum | 1 Gy iron | DP, 1 Gy |
| d33 | Control | Sham | CD, Sham |
| d34 | Control | 1 Gy iron | CD, 1 Gy |
| d35 | Dried Plum | Sham | DP, Sham |
| d36 | Dried Plum | 1 Gy iron | DP, 1 Gy |
| d37 | Control | Sham | CD, Sham |
| d38 | Control | 1 Gy iron | CD, 1 Gy |
| d39 | Dried Plum | Sham | DP, Sham |
| d40 | Dried Plum | 1 Gy iron | DP, 1 Gy |

Appendix D: Bone Homogenization and Total RNA Extraction Protocol*

*Materials and methods derived from “Total RNA Extraction Using Trizol” protocol as provided by Dr. Ann-Sofie Schreurs

TITLE Bone Homogenization and Total RNA Extraction

PURPOSE To homogenize bone samples and perform extraction of RNA from these samples

MATERIALS

Lab supplies:

| | |
|-----------------------------------|----------------------------------|
| Bucket of crushed ice | Tube racks |
| Centrifuge that can be set to 4°C | 15mL conical tube |
| Aluminum foil | P1000 and P200 pipettes and tips |
| Scalpel | RNase ZAP |
| Tweezers | Small petri dishes |
| Homogenizer | 2mL tubes |

Reagents:

RNase-free water
Bone samples
Trizol
Chloroform
70% Ethanol

METHODS

Perform homogenization in the chemical hood with proper PPE due to the use of toxic chemicals.

- 1) Remove bones from freezer and allow to thaw on ice for ~30 minutes prior to time of homogenization.
- 2) Clean all surfaces and pipettes with RNase ZAP.
- 3) Lie out aluminum foil in the fume hood and prepare necessary scalpel, tweezers, and petri dishes. All should be cleaned with RNase ZAP before use.
- 4) Fill a 15mL conical tube with RNase-free water to clean tip of homogenizer.
- 5) Set centrifuge to cool to 4C to be ready during later part of protocol.
- 6) Run the homogenizer in water on medium to high setting for 10-15 seconds. Remove any leftover pieces of tissue you may see with tweezers and clean with RNase ZAP.
- 7) Label 2mL tubes and fill them with 500uL of Trizol.
- 8) Take out on piece of thawed bone and place on a petri dish. Clean off any excess tissue around the bone and use a scalpel to cut the bone into 3-4 small pieces. Place bone pieces into appropriately labeled tubes with Trizol.
- 9) Homogenize at a moderate rate and increase slowly for approximately 30-60 seconds, until all fragments are a fine powder.

- 10) Add an additional 500uL of Trizol to each tube to bring final volume to 1mL.
- 11) Discard petri dish between bones and clean homogenizer in water after each consecutive sample. Make sure all possible pieces of bone tissue are cleaned off from tip of homogenizer.
- 12) Once homogenization of all bone samples is complete, spin down all tubes at 12,000g for 10 minutes at 4C. Remove supernatant, transferring half and half of it to two labeled tubes.
- 13) Bring the final volume to each respective tube to 1mL with excess Trizol to dilute calcium
- 14) Incubate for 5 minutes at room temperature.
- 15) Add 200uL of chloroform to each 1mL Trizol tube. Place another rack, on top of your tubes, sitting in another rack, in order to shake all tubes at once, and shake vigorously for 15 seconds.
- 16) Incubate at room temperature for 3 minutes.
- 17) Centrifuge samples at 12,000g for 12 minutes at 4C. After centrifugation, you should see that the sample is settling into 3 layers/phases. *Note: bottom red organic phase is protein, the intermediate phase is DNA, and the clear aqueous phase is RNA.*
- 18) Transfer the aqueous phase to a new 2mL tube being very cautious not to take up any of the intermediate, DNA phase. Remove in 200uL aliquots, if appropriate. Combine the aqueous phases of the two separate aliquots from step 12 into the same tube.
- 19) Slowly add equal volume of 70% ethanol to the aqueous phase or the necessary volume to bring the final volume to 2 mL. Mix the tube gently by inversion.
- 20) Continue on to the total RNA cleanup protocol.

Appendix E: Cleanup of Total RNA Protocol*

*Materials and methods derived from “Cleanup of total RNA with RNeasy mini kit” protocol as provided by Dr. Ann-Sofie Schreurs

TITLE Cleanup of Total RNA

PURPOSE To cleanup Total RNA samples after RNA extraction with RNeasy mini kit in preparation for conversion to cDNA

MATERIALS

Lab supplies:

1.5mL collection tubes

P1000, P200, P100, P1 and tips

Spectrophotometer (NanoDrop, Wilmington, DE, USA)

Bioanalyzer (Agilent Technologies, Santa Clara, CA, USA)

Reagents:

RNeasy mini kit (Qiagen, Inc., Valenica, CA, USA)

METHODS

- 1) After RNA extraction, transfer 700uL of RNA sample into an RNeasy mini column placed inside a 2mL collection tube. Centrifuge at 10,000rpm for 30 seconds and discard flow-through. Repeat until all extracted RNA sample has been run through the RNeasy mini column.
- 2) Add 350uL of Buffer RW1 into RNeasy mini column and centrifuge at 10,000rpm for 30 seconds. Discard flow-through.
- 3) Prepare DNase I from stock (stored in 4C fridge) by dissolving it in 550uL of RNase-free water. Do not vortex. Prepare 10uL of DNase I stock solution with 70uL Buffer RDD per sample.
- 4) Pipette 80uL of DNase I incubation mix directly onto the RNeasy gel membrane and let it incubate on bench top for 15 minutes.
- 5) Pipette 350uL of Buffer RW1 into the RNeasy column, and centrifuge at 10,000rpm for 30 seconds. Discard flow-through.
- 6) Transfer RNeasy column to new 2mL collection tube. Pipette 500uL of Buffer RPE in the RNeasy column. Centrifuge at 10,000rpm for 30 seconds. Discard flow-through.
- 7) Add another 500uL of Buffer RPE to the RNeasy column. Centrifuge at 10,000rpm for 2 minutes. Discard flow-through.
- 8) To eliminate any remnants of Buffer RPE, centrifuge again at 13,00rpm for 1 minute.
- 9) Transfer RNeasy column to a new 1.5mL collection tube. Pipette 30uL RNase-free water directly to the RNeasy gel membrane. Wait 5 minutes and then centrifuge at 10,000rpm for 1 minute.
- 10) Determine RNA quantity using a spectrophotometer with 1uL of sample.
- 11) Confirm quality of RNA using a 2100 Bioanalyzer.
- 12) Store all samples in -80C freezer until use.

Appendix F: Preparation of total RNA samples Protocol

TITLE Preparation of total RNA samples prior to cDNA conversion

PURPOSE To prepare total RNA samples to equal RNA concentrations prior to conversion to cDNA

MATERIALS

Lab supplies:

1.5mL micro-centrifuge tubes

Spectrophotometer (NanoDrop, Wilmington, DE, USA)

Reagents:

RNA samples

RNase-free water

METHODS

After determining the concentration of all RNA samples, compare concentrations and if there is much variation, dilute all samples to 150ng/uL.

- 1) Calculate new volume of RNA necessary for dilution to 150ng/uL, with a final volume of 10uL. Equation used: $(150 \times 10) / (\text{initial RNA concentration})$
- 2) Calculate new volume of water to mix with RNA. Equation used: $10 - (\text{new volume of RNA})$.
- 3) Prepare diluted sample mixtures.
- 4) Determine new RNA quantity using a spectrophotometer.

Appendix G: cDNA Protocol*

*Materials and methods derived from “cDNA Synthesis” Protocol as provided by Candice Tahimic

TITLE Conversion of RNA to cDNA

PURPOSE Conversion of RNA samples to cDNA in preparation for qPCR

MATERIALS

Lab supplies:

PCR tubes
Ice block for PCR tubes
P200, P100, and P20 plus tips
Thermocycler

Reagents:

| | |
|---------------------|-----------------------|
| Diluted RNA samples | 5X Standard Buffer |
| RNase-free water | DTT |
| Random Hexamers | RNase Out |
| dNTPs | Reverse Transcriptase |

METHODS

- 1) Thaw diluted RNA samples (all ~150ng/uL)
- 2) Prepare standard cDNA reaction mixtures for 15ng RNA/uL
 - a. Volume of RNA per reaction is determined by $(15 \times \text{total reaction volume}) / [\text{RNA}]$
 - b. Volume of Water per reaction is determined by $(6 - \text{volume of RNA})$
- 3) Prepare master mix 1: 0.75uL of Random Hexamers and 0.75uL of dNTPS per 1 reaction.
- 4) Add 1.5uL of master mix 1 to all RNA+water preps (keep all solutions on ice block)
- 5) Heat solutions in thermocycler for 5 minutes at 65C and then quickly put back on ice block
- 6) Prepare master mix 2: 1.5uL of diWater, 3uL of 5X First Standard Buffer, 1.5uL of DTT, and 0.75uL of RNase Out per 1 reaction
- 7) Add 6.75uL to each tube and gently pipette-mix
- 8) Put in thermocycler for 2 minutes at 37C
- 9) Remove samples and put on ice block
- 10) Add 0.75uL of Reverse Transcriptase to each sample. Mix gently.
- 11) Put samples in thermocycler for following cycles:
 - a. 25C for 10 minutes
 - b. 37C for 50 minutes
 - c. 70C for 15 minutes
 - d. 4C dwell
- 12) Store cDNA in -80C freezer until use

Appendix H: Qualitative Polymerase Chain Reaction (qPCR) Protocol*

*Materials and methods derived from “qPCR” Protocol as provided by Dr. Ann-Sofie Schreurs

TITLE Gene expression by qPCR

PURPOSE To determine expression level of gene of interest in cDNA samples

MATERIALS

Lab supplies:

7300 RT-PCR System (Applied Biosystems, Foster City, CA, USA)

96 well plate

384 well plate

P1000, P200, P20 and tips

Multi-channel pipette (8 channels)

Aluminum foil

MicroAmp Optical Adhesive Film (PCR compatible)

Reagents:

cDNA samples

RNase-free water

Taqman gene expression primers for GOI and Housekeeping Gene

GoTaq® RT-qPCR System (Promega, Madison, WI, USA)

METHODS

- 1) Follow excel file below to calculate necessary amounts of reagents for a desired number of genes and a specific number of samples.
- 2) Thaw cDNA samples on ice as well as RNase-free water.
- 3) Thaw appropriate primers for GOI and housekeeping gene. *Primers are light sensitive so always keep covered with foil.*
- 4) Prepare Mix B, Part 1 in a 1.5mL micro-centrifuge tube. Follow “recipe” from figure 23.
- 5) For Part 2, aliquot the appropriate amount of Part 1 into a 96 well plate. Number of aliquots will be determined by the number of samples you have. Prepare the 96 well plate as depicted in figure 24.
- 6) Then aliquot the appropriate amount of cDNA into the wells from part 5 based on sample number.
- 7) Using a multichannel pipette (8 tips), pipette 7.5uL of samples from part 2 into the 365 well plate. Prepare the 384 well plate as depicted in figure 24. Cover the plate with plastic cover slip when not being used.
- 8) Prepare Mix A for each of your primers.

- 9) Aliquot 22.2uL of Mix A into 8 consecutive wells of the 96 well plate.
- 10) Again, using the multi-channel pipette, aliquot 2.5uL of aliquoted Mix A from part 9 and add to samples in the 384 well plate from part 7. Pipette mix.
- 11) Cover slide with optical adhesive film.
- 12) Take to 7300 RT-PCR System machine (Applied Biosystems, Foster City, CA, USA) and run the accompanied program for appropriate number of samples and 10uL reaction volume/well.

| Mix A for L19 VIC and Gene of Interest (GOI) FAM | | Rxns (10 uL total/rxn) | |
|--|---------------|---|-------------|
| Number of Samples | | 31 | |
| Number of Genes | | 1 | |
| Mix A (1 per GOI) | | | |
| Number of cDNA samples x 2 plus 15% margin | | 71 | |
| | 1 | 71 | |
| DW | 1.5 | 106.5 | |
| Primers + Probe (20X) GOI, FAM | 0.5 | 35.5 | |
| L19 Housekeeping gene (20X), VIC | 0.5 | 35.5 | |
| TOTAL | 2.5 uL | 177.5 | |
| Aliquot | 22.2 | uL into 8 wells | |
| Mix B (Mastermix for each cDNA for all genes) | | | |
| Part 1: Create DW + Mastermix for all Reactions | | | |
| DW | 163.7 | uL | *10% Margin |
| Mastermix | 409.2 | uL | |
| Total | 572.9 | uL | |
| Part 2: Create MM for each cDNA | | | |
| Number of primers to be used X 2 plus 20% margin | | 2.4 | |
| | | <i>Aliquot from part 1 into 96 well plate</i> | |
| | 1 | 2.4 | 2.4 |
| DW from Mix B (Part 1) | 2 | 4.8 | 16.8 |
| PCR Mastermix from Mix B (Part 1) | 5 | 12 | |
| cDNA | 0.5 | 1.2 | 1.2 |
| | 7.5 uL | | 18 |

Figure 23. Excel spreadsheet utilized to calculate qPCR "recipe" for 31 samples and 1 gene of interest. Orange highlighted boxes indicate the mixes that need to be made, Mix A, Mix B (Part 1), and Mix B (Part 2). Yellow highlighted boxes indicate the number of uL that will be aliquoted from the 96 well plate into the 384 well plate. Final volume in each well (384 well plate) should be 10uL.

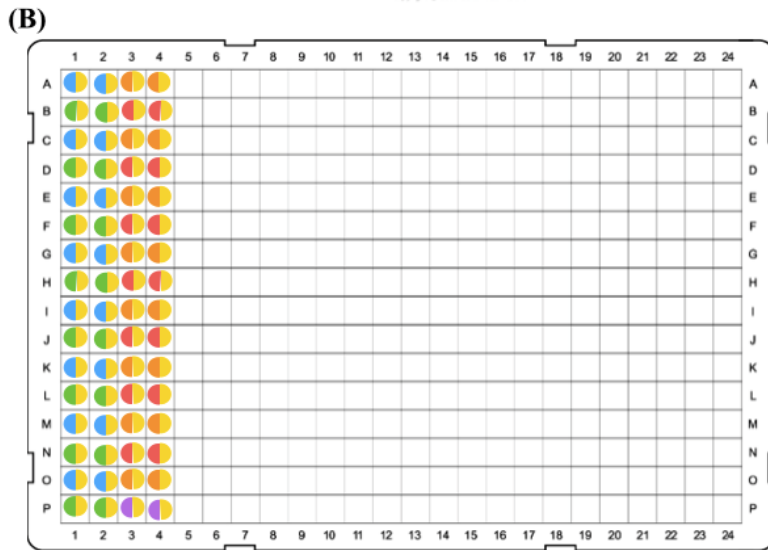
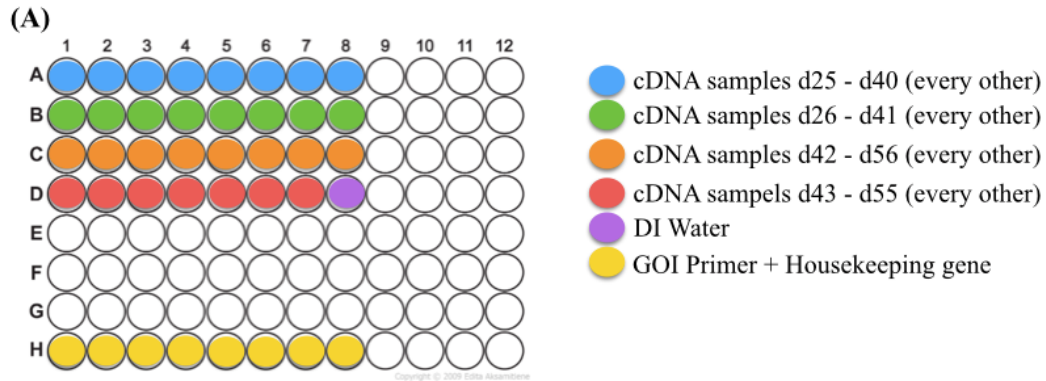


Figure 24. Set up for the 96 well and 384 well plates utilized for qPCR of 31 samples and 1 gene of interest from the ‘Dried plum + 2Gy gamma’ experiment. (A) 96 well plate of Mix B (Part 2) in each well = cDNA gets combined with Mix B (Part 1). (B) 384 well plate where 7.5uL of Mix B (Part 2) is combined per well with 2.5uL of Mix A (specific to one gene).

Appendix I. Table of Genes Analyzed

Table 5. Table of all genes we analyzed during the course of our project during the gene expression phase.
Table includes full names for our genes of interest as well as a description of their functions.

| Gene | Full Name | Category | Description/Function | Assay ID# |
|-------------------|---|---------------------------------|---|---------------|
| Bglap | Bone gamma-carboxylglutamate protein | Bone formation | Secreted by osteoblasts that regulates bone remodeling and energy metabolism | Mm03413826 |
| BMP-2 | Bone morphogenetic protein 2 | Bone formation | Induce osteoblast differentiation | Mm01340178_m1 |
| BMP-4 | Bone morphogenetic protein 4 | Bone formation | Stimulation of osteoblast activity | Mm00432087_m1 |
| Cdkn1a/p21 | Cyclin-dependent kinase inhibitor 1A | Oxidative stress | It prevents phosphorylation of cdk's and blocks the cell cycle in response to DNA damage | Mm04205640_g1 |
| FOXO3 | Forkhead Box O3 | Oxidative stress | Transcriptional activator, which triggers apoptosis under situations of oxidative stress | Mm01185722_m1 |
| Gadd45a | Growth Arrest and DNA-Damage-Inducible, Alpha | Oxidative stress | Increased in response to stressful growth arrest conditions or after exposure to DNA-damaging agents | Mm00432802_m1 |
| IGF1 | Insulin like growth factor 1 | Bone formation | Critical mediator of bone growth | Mm00439560_m1 |
| mTOR | Mechanistic Target of Rapamycin (Ser/Thr Kinase) | Oxidative Stress | Encodes a protein kinase that mediates cell responses to certain stresses, namely DNA damage and nutrient deprivation | Mm00444968_m1 |
| Nfatc1 | Nuclear Factor of Activated T-Cells, Cytoplasmic, Calcineurin-Dependent 1 | Bone resorption (inhibition) | | Mm00479445_m1 |
| Nfe2l2 | Nuclear factor (erythroid-derived 2)-like 2 (Nrf2) | Oxidative stress | Involved in the protection against oxidative damage due to injury or other inflammation. | Mm00477784_m1 |
| Opg | Osteoprotegerin | Bone resorption (inhibition of) | As a competitive inhibitor, works to prevent bone resorption. | Mm01205928_m1 |
| Postn | Periostin | Bone formation | Essential for bone remodeling | Mm01284919_m1 |
| Rankl | Receptor activator of nuclear factor kappa-B ligand | Bone resorption | Its surface bound molecule (CD254) is believed to activate osteoclasts and thus bone resorption activity. | Mm00441906_m1 |
| Runx2 | Runt-Related Transcription Factor 2 | Bone formation | This protein is regarded as essential for osteoblastic differentiation | Mm00501584_m1 |
| SOD1 | Superoxide Dismutase 1, Soluble | Oxidative stress | Encoded protein responsible for destroying free superoxide radicals, thus protects against oxidative damage | Mm01344233_g1 |
| SOST | Sclerostin | Bone resorption | Produced by osteocytes and inhibits bone formation | Mm04208528_m1 |
| TP53 | Tumor Protein P53 | Oxidative stress | Induce cell cycle arrest, apoptosis, senescence, DNA repair in response to cellular stresses | Mm01731290_g1 |

Appendix J. TBARS Assay Protocol*

*Materials and methods derived from Bone and Signaling Lab, NASA ARC.

TITLE TBARS Assay

PURPOSE To measure MDA levels in serum, bone supernatant, or bone pellet samples.

MATERIALS

Lab supplies:

BioTek Plate Reader

96 well plate (black)

P1000, P200, P20 and tips

Multi-channel pipette (8 channels)

Aluminum foil

Reagents:

Thiobarbituric Acid Assay Reagent

TBA Acetic Acid

Sodium Hydroxide Assay Reagent

TBA Malondialdehyde Standard

TCA Assay Reagent

METHODS

Color Reagent Preparation

- 1) TBA Acetic Acid and Sodium Hydroxide reagent were diluted with 40 ml of HPLC-grade water. That is, 10 ml of each of these reagents was added to 40 ml of HPLC grade-water in separate 50 ml tubes.
- 2) 45 samples were assumed when preparing the volume of the color reagent. To this end, 18.72 ml of Acetic Acid Solution were mixed with 18.72 ml of Sodium hydroxide in a separate 50 ml beaker.
- 3) 198.72 mg of TBA reagent were weighed and added to the beaker, along with a stir bar. The contents of the beaker were stirred until the dissolution of the solid TBA, as much as possible or until the powder was uniform and as few larger chunks were visible.

Fluorometric Standard Preparation

- 1) 25 μ l of MDA Standard were mixed with 975 μ l of water to obtain a stock solution of 12.5 μ M.
- 2) 8 glass test tubes were labeled A-H.
- 3) Each of eight tubes was prepared according to the following table, to create the MDA fluorometric standards.

| Tube | MDA (μl) | Water (μl) | MDA Concentration (μM) |
|------|-----------------------|-------------------------|-------------------------------------|
| A | 0 | 1000 | 0 |
| B | 5 | 995 | 0.0625 |
| C | 10 | 990 | 0.125 |
| D | 20 | 980 | 0.25 |
| E | 40 | 960 | 0.5 |
| F | 80 | 920 | 1 |
| G | 200 | 800 | 2.5 |
| H | 400 | 600 | 5 |

TBARS Assay

- 1) 1.5 ml centrifuge tube was labeled for each sample.
- 2) 100 μl of sample or standard added to appropriate tube.
- 3) 100 μl of TCA Assay Reagent was added to the tube and swirled to mix.
- 4) 800 μl of Color Reagent was added to each tube and vortexed.
- 5) Tubes were added to boiling water and left to boil for 1 hour.
- 6) After 1 hour, tubes were immediately transferred to an ice bath to stop the reaction.
- 7) Samples were incubated on ice for 10 minutes.
- 8) Tubes were centrifuged at 1,600 g and 4°C for 10 minutes.
- 9) Because the tubes are stable at room temperature for 30 minutes, the following had to be performed expediently.
 - a. 200 μl of solution from each tube was transferred in duplicate to a black, 96-well plate.
 - b. A plate reader was used to read the fluorescence at an excitation wavelength of 530 nm and an emission wavelength of 550 nm. Excitation and emission bandwidths were set to no higher than 10 nm.

Appendix K. Table of microCT Parameters of Interest [23]

Table 6. Table of all parameters of interest that were analyzed after performing microCT for all vertebrae samples.

| Abbreviation | Full Name | Description | Standard Unit |
|---------------|-----------------------|---|-------------------|
| BV/TV | Bone volume fraction | The ratio of bone volume to total volume of region of interest | % |
| Tb.Th | Trabecular Thickness | The average thickness of trabeculae | mm |
| Tb.Sp | Trabecular Separation | The average separation lengths between trabeculae | mm |
| Tb.N | Trabecular Number | The average number of trabeculae within region of interest | 1/mm |
| Conn.D | Connectivity Density | “A measure of the degree of connectivity of trabeculae normalized by total volume (TV)” | 1/mm ³ |
| SMI | Structure model index | “An indicator of the structure of trabeculae; SMI will be 0 for parallel plates and 3 for cylindrical rods” | 1/mm |

12. References

1. Reisz, Julie A., Nidhi Bansal, Jiang Qian, Weiling Zhao, and Cristina M. Furdul. "Effects of Ionizing Radiation on Biological Molecules—Mechanisms of Damage and Emerging Methods of Detection." *Antioxidants & Redox Signaling* 21.2 (2014): 260-92. Print.
2. Willey, Jeffrey S., Shane A. J. Lloyd, Gregory A. Nelson, and Ted A. Bateman. "Ionizing Radiation and Bone Loss: Space Exploration and Clinical Therapy Applications." *Clinic Rev Bone Miner Metab Clinical Reviews in Bone and Mineral Metabolism* 9.1 (2011): 54-62. Print.
3. Kondo, H., K. Yumoto, J. S. Alwood, R. Mojarrab, A. Wang, E. A. C. Almeida, N. D. Searby, C. L. Limoli, and R. K. Globus. "Oxidative Stress and Gamma Radiation-induced Cancellous Bone Loss with Musculoskeletal Disuse." *Journal of Applied Physiology* 108.1 (2009): 152-61. Web.
4. Barcellos-Hoff, Mary Helen, Eleanor A. Blakely, Sandeep Burma, Albert J. Fornace, Stanton Gerson, Lynn Hlatky, David G. Kirsch, Ulrike Luderer, Jerry Shay, Ya Wang, and Michael M. Weil. "Concepts and Challenges in Cancer Risk Prediction for the Space Radiation Environment." *Life Sciences in Space Research* 6 (2015): 92-103. Print.
5. Karsenty, Gerard. "The Complexities of Skeletal Biology." *Nature* 423 (2003): 316-18. Print.
6. Norman, Stephanie C., David W. Wagner, Gary S. Beaupre, and Alesha B. Castillo. "Comparison of Three Methods of Calculating Strain in the Mouse Ulna in Exogenous Loading Studies." *Journal of Biomechanics* 48 (2015): 53-58. Print.
7. Franklin, M., S.y. Bu, M.r. Lerner, E.a. Lancaster, D. Bellmer, D. Marlow, S.a. Lightfoot, B.h Arjmandi, D.j. Brackett, E.a. Lucas, and B.j. Smith. "Dried Plum Prevents Bone Loss in a Male Osteoporosis Model via IGF-I and the RANK Pathway." *Bone* 39.6 (2006): 1331-342. Web.
8. Rendina, Elizabeth, Kelsey D. Hembree, Mckale R. Davis, Denver Marlow, Stephen L. Clarke, Bernard P. Halloran, Edralin A. Lucas, and Brenda J. Smith. "Dried Plum's Unique Capacity to Reverse Bone Loss and Alter Bone Metabolism in Postmenopausal Osteoporosis Model." *PLoS ONE* 8.3 (2013): n. pag. Web.
9. Drake, Matthew T., Bart L. Clarke, and Sundeep Khosla. "Bisphosphonates: Mechanism of Action and Role in Clinical Practice." *Mayo Clinic Proceedings* 83.9 (2008): 1032-045. *NIH Public Access*. Web.
10. Kennel, Kurt A., and Matthew T. Drake. "Adverse Effects of Bisphosphonates: Implications for Osteoporosis Management." *Mayo Clinic Proceedings* 84.7 (2009): 632-38. Web.
11. Schreurs, A.-S., Y. Shirazi-Fard, M. Shahnazari, J. S. Alwood, T. A. Truong, C. G. T. Tahimic, C. L. Limoli, N. D. Turner, B. Halloran, and R. K. Globus. "Dried plum diet protects from bone loss caused by ionizing radiation." *Sci. Rep. Scientific Reports* 6 (2016): 21343. *Scientific Reports*. Web. 19 Feb. 2016.
12. Nishio, K., A. Tanabe, R. Maruoka, K. Nakamura, M. Takai, T. Sekijima, S. Tunetoh, Y. Terai, and M. Ohmichi. "Bone Mineral Loss Induced by Anticancer Treatment for Gynecological Malignancies in Premenopausal Women." *Endocrine Connections* 2.1 (2012): 11-17. Web.
13. Chen, Jin-Ran, Oxana P. Lazarenko, Jian Zhang, Michael L. Blackburn, Martin Jj Ronis, and Thomas M. Badger. "Diet-Derived Phenolic Acids Regulate Osteoblast and Adipocyte Lineage Commitment and Differentiation in Young Mice." *J Bone Miner Res Journal of Bone and Mineral Research* 29.5 (2014): 1043-053. Web.
14. Bu, So Young, Tamara S. Hunt, and Brenda J. Smith. "Dried Plum Polyphenols Attenuate the Detrimental Effects of TNF- α on Osteoblast Function Coincident with Up-regulation of Runx2, Osterix and IGF-I." *The Journal of Nutritional Biochemistry* 20 (2008): 35-44. Print.
15. Bu, So Young, Megan Lerner, Barbara J. Stoecker, Emily Boldrin, Daniel J. Brackett, Edralin A. Lucas, and Brenda J. Smith. "Dried Plum Polyphenols Inhibit Osteoclastogenesis by Downregulating NFATc1 and Inflammatory Mediators." *Calcified Tissue International Calcif Tissue Int* 82.6 (2008): 475-88. Print.
16. Hooshmand, Shirin, Ajay Kumar, Ji Yao Zhang, Sarah A. Johnson, Sheau C. Chai, and Bahram H. Arjmandi. "Evidence for Anti-inflammatory and Antioxidative Properties of Dried Plum Polyphenols in Macrophage RAW 264.7 Cells." *Food & Function* 6.5 (2015): 1719-725. Print.
17. Sacco, Sandra Maria, Marie-Noëlle Horcajada, and Elizabeth Offord. "Phytonutrients for Bone Health during Ageing." *British Journal of Clinical Pharmacology Br J Clin Pharmacol* 75.3 (2012): 697-707. Print.
18. Johnson, Catherine D., Edralin A. Lucas, Shirin Hooshmand, Sara Campbell, Mohammed P. Akhter, and Bahram H. Arjmandi. "Addition of Fructooligosaccharides and Dried Plum to Soy-Based Diets Reverses

- Bone Loss in the Ovariectomized Rat." *Evidence-Based Complementary and Alternative Medicine* 836267 (2011): 1-7. Print.
19. Heino, Terhi, and Teuvo Hentunen. "Differentiation of Osteoblasts and Osteocytes from Mesenchymal Stem Cells." *CSCR Current Stem Cell Research & Therapy* 3.2 (2008): 131-45. Web.
 20. Udagawa, N., N. Takahashi, T. Akatsu, H. Tanaka, T. Sasaki, T. Nishihara, T. Koga, T. J. Martin, and T. Suda. "Origin of Osteoclasts: Mature Monocytes and Macrophages Are Capable of Differentiating into Osteoclasts under a Suitable Microenvironment Prepared by Bone Marrow-derived Stromal Cells." *Proceedings of the National Academy of Sciences* 87.18 (1990): 7260-264. Web.
 21. Mylonas, C., and D. Kouretas. "Lipid Peroxidation and Tissue Damage." *In Vivo* 13.3 (1999): 295-309. *NCBI PubMed*. Web. 20 May 2016.
 22. *TBARS (TCA Method) Assay Kit*. Ann Arbor: Cayman Chemical, 2014. Print.
 23. Bouxsein, Mary L., Stephen K. Boyd, Blaine A. Christiansen, Robert E. Guldberg, Karl J. Jepsen, and Ralph Müller. "Guidelines for Assessment of Bone Microstructure in Rodents Using Micro-computed Tomography." *J Bone Miner Res Journal of Bone and Mineral Research* 25.7 (2010): 1468-486. Web.
 24. Hooshmand, S., M. Kern, D. Metti, P. Shamloufard, S. C. Chai, S. A. Johnson, M. E. Payton, and B. H. Arjmandi. "The Effect of Two Doses of Dried Plum on Bone Density and Bone Biomarkers in Osteopenic Postmenopausal Women: A Randomized, Controlled Trial." *Osteoporosis International Osteoporos Int* (2016): 1-9. *Springer*. Web. Epub ahead of print.
 25. <http://www.spineuniverse.com/conditions/back-pain/low-back-pain/lumbar-spine-surgery-will-you-need-surgery-your-lower-back-pain>